Grid Peeling of Parabolas

Moritz Rüber, Morteza Saghafian, Günter Rote*

February 27, 2024

Abstract

Grid peeling is the process of repeatedly removing the convex hull vertices of the grid points that lie inside a given convex curve. It has been conjectured that, for a more and more refined grid, grid peeling converges to a continuous process, the *affine curve-shortening flow*, which deforms the curve based on the curvature.

We prove this conjecture for one class of curves, parabolas with a vertical axis, and we determine the value of the constant factor in the formula that relates the two processes.

Contents

*The authors are listed by seniority. Authors' addresses and affiliations: M. R. and G. R.: Freie Universität Berlin, m.rueber@web.de and rote@inf.fu-berlin.de. M. S.: ISTA (Institute of Science and Technology Austria), Klosterneuburg, Austria, Morteza.Saghafian@ist.ac.at.

1 Introduction

In 2017, Eppstein, Har-Peled, and Nivasch [9] observed a remarkable connection between a continuous deformation of a curve in the plane, the *affine curve-shortening flow* (ACSF), and a discrete process, *grid peeling*.

In the affine curve-shortening flow, a smooth curve is deformed by moving every point toward the direction in which the curve bends, at a speed of $\kappa^{1/3}$ in the normal direction, where κ is the curvature at that point at the current point of time, see Figure 1. The left part of Figure 2 shows a few snapshots of this inward-growing process, starting from a semicircle. (The semicircle is not a smooth curve, but the definition of the flow can be extended to cover piecewise smooth curves.)

By contrast, grid peeling is a process that is discrete both in space and in time. Given a convex curve, we start by finding the convex hull of all points of a uniform square grid inside the curve. Then we iteratively remove the vertices of the convex hull, and take the convex hull of the remaining grid points.

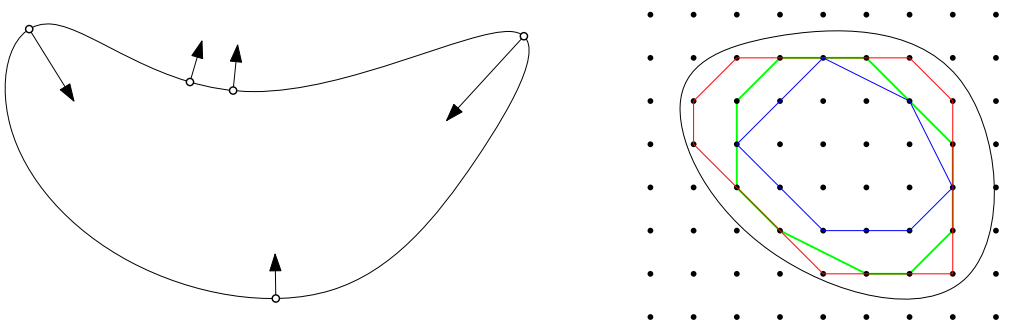

Figure 1: Left: The Affine Curve-Shortening Flow (ACSF). The velocity is indicated by arrows, whose length is proportional to $\kappa^{1/3}$. Right: A convex curve and the first three steps of grid peeling.

Eppstein, Har-Peled, and Nivasch observed that, as the underlying grid is refined, grid peeling approximates the ACSF process, as can be seen in Figure 2. More specifically, they conjectured that, for a more and more refined grid of spacing $1/n$, the m-th convex layer of a convex curve converges to the ACSF after time T, if m is chosen as

$$m = \lfloor c_{\mathrm{g}} T n^{4/3} \rfloor \tag{1}$$

for an appropriate constant c_{g}, which was experimentally determined to be approximately 1.6 [9, Conjecture 1].

We prove this conjecture for the special case when the curve is a parabola with vertical axis, and we find the precise value of the constant c_{g}:

$$c_{\mathrm{g}} = \sqrt[3]{\frac{\pi^2}{2\zeta(3)}} \approx 1.60120980542577, \tag{2}$$

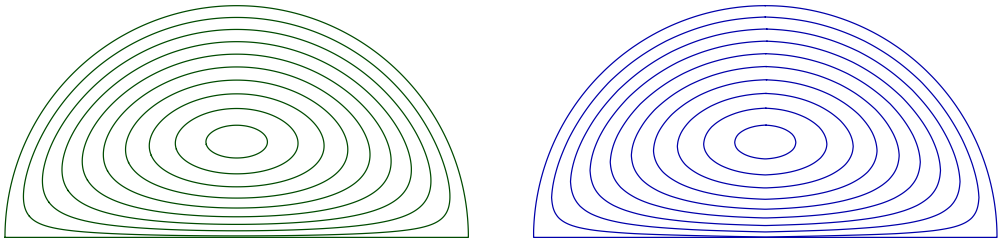

Figure 2: ACSF (left) and grid peeling (right) of a semicircle of diameter 1. The left figure shows 10 snapshots of ACSF with regular time increments; the right figure shows every 2714th convex layer for a grid of spacing 1/5000. The increment 2714 corresponds to the conjectured formula (1) with a value $c_{\mathrm{g}} \approx 1.587$. (From [9, Figure 3], by permission from the authors.)

where

$$\zeta(s) = 1 + \frac{1}{2^s} + \frac{1}{3^s} + \frac{1}{4^s} + \cdots$$

is the Riemann zeta function, with values $\zeta(2) = \pi^2/6 \approx 1.644934$ and $\zeta(3) \approx 1.2020569$.

Theorem 1. *For the parabola* $\Pi\colon y = ax^2/2 + bx + c$*, the ACSF is a vertical translation with velocity* $a^{1/3}$*. Thus, at time* $T > 0$*, it becomes the parabola* $\Pi^T\colon y = ax^2/2 + bx + c + Ta^{1/3}$*.*

If we apply grid peeling to Π *with a grid of spacing* $1/n$ *for* $m = \lfloor c_{\mathrm{g}} T n^{4/3} \rfloor$ *steps, then, as* $n \to \infty$*, the vertical distance between the resulting grid polygon and* Π^T *is bounded by*

$$O\left(\frac{(Ta^{2/3} + a^{-2/3}) \log \frac{n}{a}}{n^{1/3}}\right).$$

For fixed T and a, this error bound goes to 0 as $n \to \infty$.

We can extend this theorem to any parabola whose axis has a rational slope a/b: A unimodular transformation with a suitable matrix $\left(\begin{smallmatrix} a & -b \\ u & v \end{smallmatrix}\right)$ of determinant 1 will leave the grid unchanged and make the axis vertical, and then Theorem 1 can be applied.

1.1 History and background

The ACSF process was first studied in the 1990s in the area of computer vision and image processing, by Alvarez, Guichard, Lions, and Morel [1] and by Sapiro and Tannenbaum [16]. One way to understand the ACSF is to regard it as a limit of *affine erosions*, as shown by F. Cao [7, Theorem 6.22]. An affine erosion with parameter ε removes the union of all pieces of area ε that can be cut off by a straight line. (In convex geometry, this is also called the *wet part*; it plays a role in estimating the area and the number of vertices of the convex hull of a random sample of points [4, 3].) Repeating this process makes the shape rounder and rounder, like a pebble rolling in water. Letting ε go to zero leads to the ACSF as the continuous limit.

The other process that we study is formed by the *convex layers* or *onion layers* of a point set. They have their origin in computational geometry and statistics: The innermost convex layer provides a robust estimate of the "center" of a distribution. The special case where the point set is a grid was first investigated by Har-Peled and Lidický [10], who showed that the $n \times n$ square grid has $\Theta(n^{4/3})$ convex layers. For a box in three and higher dimensions, the asymptotic number of layers is not known, see for example [8] and the references given there. See [2, 6, 7] for more background and references to the literature, both on the ACSF and on grid peeling.

1.1.1 Peeling with random sets

More recently, Calder and Smart [6] investigated the related process where the grid is replaced by a random point set. More precisely, the refined grid of spacing $1/n$ is replaced by a Poisson point set of density $1/n^2$. In this setting, they could prove an analogous statement:

There exists a constant $c_r \approx 1.3$ such that the m-th convex layer, for $m = \lfloor c_r T n^{4/3} \rfloor$, approximates the ACSF at time T. Since the underlying process is random, this statement requires some probabilistic qualification; see [6, Theorem 1.2] for the precise statement, which is quite strong and general: It is valid in arbitrary dimension, and convergence holds (with high probability) uniformly for all T. The density can be nonuniform, which corresponds to an ACSF with a location-sensitive speed. There is no precise formula for the value of the random-set peeling constant c_r, not even a conjectured one. Since $c_r < c_g$, random-set peeling proceeds faster than grid peeling at the same density.

1.1.2 Homotopic curve shortening

Avvakumov and Nivasch [2] extended peeling to nonconvex and even self-crossing curves, introducing the concept of *homotopic curve shortening*. Both for grid peeling and for random-set peeling, the observed relation with the ACSF process persists also in this setting.

1.1.3 Equivariance under affine transformations

It is easy to check that the ACSF is equivariant under area-preserving affine transformations, a property that gave rise to the term "*affine* curve-shortening flow." (Arbitrary affine transformations, which are not necessarily area-preserving, can be accommodated by scaling the time parameter.) The relation between ACSF and grid peeling is the more surprising as grid peeling does not have this property. Grid peeling is equivariant only under a special class of affine transformations, namely those that also preserve the grid (unimodular transformations), a property that we will often use. (Peeling with random sets, on the other hand, is clearly equivariant under area-preserving affine transformations.)

1.2 Conics

As stated in Theorem 1, the ACSF for a parabola is just a translation at constant speed. This special behavior is shared, to a certain extent, by the other types of conics: They are scaled under ACSF but otherwise maintain their shape [17, Lemma 8]. More specifically,

- an ellipse (or a circle) *shrinks* toward the center, and eventually collapses to a point;
- a parabola is *translated* parallel to the axis;
- a hyperbola *expands* from its center.

Among the conics, parabolas appear most attractive for investigation, because they don't even need to be scaled. Also for the case of random-set peeling, the peeling of a parabola lies at the core of the proof of Calder and Smart [6], forming what they call the *cell problem*. As regards experiments, the downside of parabolas, as opposed to ellipses, is that a parabola is an unbounded curve, and even the first step of grid peeling is not obvious to compute. However, as we shall see, for parabolas with rational coefficients, we can make use of a certain periodicity along the curve, which reduces grid peeling to a finite computation. Once the sequence of peelings goes into a loop, one has a complete overview of the whole infinite grid peeling process.

Grid peeling has been investigated also for *hyperbolas*, in a sense. If one starts with the upper-right quadrant $\mathbb{R}_+ \times \mathbb{R}_+$, the ACSF develops into positive branches of hyperbolas $xy = c$. Eppstein, Har-Peled, and Nivasch [9, Theorem 5] investigated the convex layers of $\mathbb{N} \times \mathbb{N}$ and proved that the m-th convex layer is sandwiched between two hyperbolas:

$$c_1 m^{3/2} \le xy \le c_2 m^{3/2}, \tag{3}$$

except that the lower bound does not hold within a strip of width $O(\sqrt{m} \log^2 m)$ around the axes.

The constants c_1 and c_2 are not computed explicitly, but some values can be worked out from the proof. We add two side remarks regarding the exception near the axes that the theorem makes. Firstly, *some* exception of this sort has to be made, because the m-th layer goes through the points $(m, 0)$ and $(0, m)$, and no hyperbola $xy = \text{const}$ can be squeezed below these points. To give the hyperbola some chance in principle to squeeze under, we might peel the quadrant of *positive* grid points, or equivalently, we allow the hyperbola to be centered at $(-1, -1)$ (or some other fixed point), but this would still not suffice for (3). Secondly, the claim [9, Theorem 5] is stated with an "exception strip" around the axes whose width is only $O(\sqrt{m})$; however, there is a small gap in the proof [9, p. 315, right column]: In the proof of Lemma 18, when applying Lemma 7 for the rectangle spanned by the points $q/2$ and q, an error term of the form $\pm O(N \log N)$ from Lemma 7 is ignored. When the error term is taken into account, the proof goes through with the larger margin of exception claimed above.

1.3 Overview

In Section 2, we define a family of specific curves, the so-called *grid parabolas* P_t. Grid peeling reproduces them with a vertical shift after t steps (or $t+1$, depending on the parity). This is our main technical result (Theorem 2), whose proof is postponed to Section 4. Based on Theorem 2, we prove Theorem 1, our main theorem about grid peeling of parabolas, in Section 3. Sections A and B analyze the quantities that arise in the construction of the grid parabola, using arguments from elementary number theory. The final Section D reports computer experiments with grid peeling for parabolas. These experiments were the source the discoveries expressed in Theorem 2 below, and its consequence, our main Theorem 1. We also describe some interesting phenomena beyond those that are discussed and proved in the first part of the paper.

2 The grid parabola

Our object of investigation is a special infinite polygonal chain P_t, which depends on a positive integer parameter t. It is defined as follows:

1. Let S_t be the set of all rational numbers $s = a/b$ with $0 < b \le t$. We call these elements the *slopes*. We will always assume that the fractions a/b representing slopes are reduced.

2. For each slope $s = a/b \in S_t$, take the longest integer vector of the form

$$\binom{x}{y} = q\binom{b}{a} \quad (q \in \mathbb{Z})$$

   with $0 < x \le t$. Let V_t denote the set of these vectors. Figure 3 shows V_t for $t = 11$.

3. Form the chain $P = P_t$ by concatenating these vectors in order of increasing slope.

Figure 4 shows a section of the grid parabola P_5.

We can make a few simple observations: It is clear that for every vector $(x, y) \in V_t$ with a positive slope, there is a corresponding vector $(x, -y) \in V_t$ with negative slope. Thus, the curve P is symmetric with respect to a vertical axis. The lowest points on P form a horizontal edge of length t. We place the origin O of our coordinate system at the center of this edge, so that the symmetry axis becomes the y-axis. When t is odd, this implies that the vertices of P have half-integral x-coordinates. Nevertheless, we will refer to the points of the square unit grid on which the vertices of P lie (as shown in Figure 4) as the *grid*.

Figure 5 applies a few grid peeling steps to the grid parabola P_5. We can see that P_5 reproduces itself after 5 iterations, translated up by 1 unit. From then on, the process repeats ad infinitum. Our central technical result is that this is always the case.

Theorem 2. *For odd t, the chain P_t repeats after t peeling steps, one unit higher.*

For even t, the chain P_t repeats after $t + 1$ peeling steps, one unit higher.

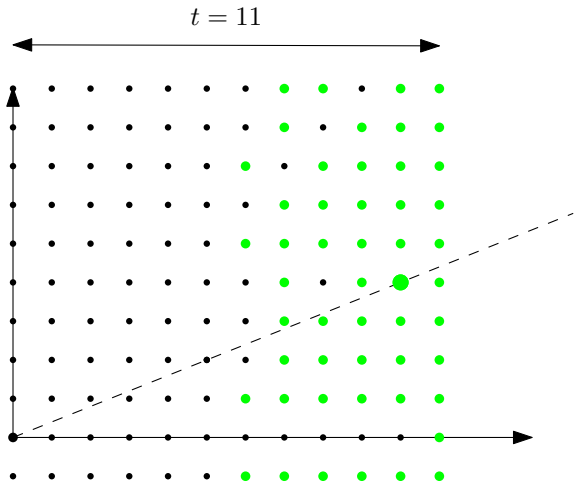

Figure 3: The set V_{11} of vectors (x, y) from which P_{11} is formed, shown as green dots. The vector with slope $s = 2/5$ is highlighted. The points of V_{11} extend indefinitely to the top and to the bottom. The picture shows the range $-1 \le y \le 9$.

Theorem 2 and the special construction of the grid parabola were suggested by experiments, which are reported in Appendix D. In Appendix C we mention that our grid parabolas play a role in the convex lattice n-gons of minimum area.

2.1 The horizontal period

While P is an infinite object, we will argue that it is sufficient to look at a finite section, because this section "repeats periodically" in a certain sense.

We partition the vectors $V_t = \cdots \cup V_t^{(-2)} \cup V_t^{(-1)} \cup V_t^{(0)} \cup V_t^{(1)} \cup V_t^{(2)} \cup \cdots$ according to the integral part of their slope into the sets

$$V_t^{(i)} := \{\, (x, y) \in S_t \mid i < \tfrac{y}{x} \le i + 1 \,\}$$

for $i \in \mathbb{Z}$. The vectors in $V_t^{(0)}$ lead P from the origin to an edge with vector (t, t) of slope 1. More precisely, in the way we have defined $V_t^{(0)}$, these vectors lead from the right endpoint of the horizontal edge to the upper-right endpoint of the edge (t, t). However, we prefer to select the midpoint of the edge (t, t), and we place a reference point Q at this point. We define the *horizontal period* H_t as the horizontal distance between the origin O and Q.

H_t is the sum of the x-coordinates of the vectors in $V_t^{(0)}$. (Only half of the vector $(t, t) \in V_t^{(0)}$ contributes to H_t, but this is compensated by including half of the vector $(t, 0) \notin V_t^{(0)}$.) The first values of H_t are $H_1, H_2, \ldots = 1, 4, 11, 22, 43, 64, 107, 150$, etc. In Section 3.1, we will evaluate this quantity and see that $H_t \approx 0.24\, t^3$ (Lemma 4).

We claim that the segment OQ has slope $\frac{1}{2}$, and therefore the y-coordinate of Q is $H_t/2$.

Proposition 1. *1. The segment OQ has slope $\frac{1}{2}$.*

2. H_t is even if and only if t is even.

Proof. The set V_t is symmetric with respect to the shearing operation $\binom{x}{y} \leftrightarrow \binom{x}{x-y}$, which keeps the "mirror line" $y = x/2$ fixed and inverts the orientation of every vertical line, see the inset of Figure 4. Thus, every vector in V_t with slope $> \frac{1}{2}$ can be matched with a vector with slope $< \frac{1}{2}$, so that the sum of these two vectors has slope $\frac{1}{2}$. The set $V_t^{(0)}$ is slightly asymmetric with respect to this mirror operation because it contains the edge of slope 1 but not the corresponding

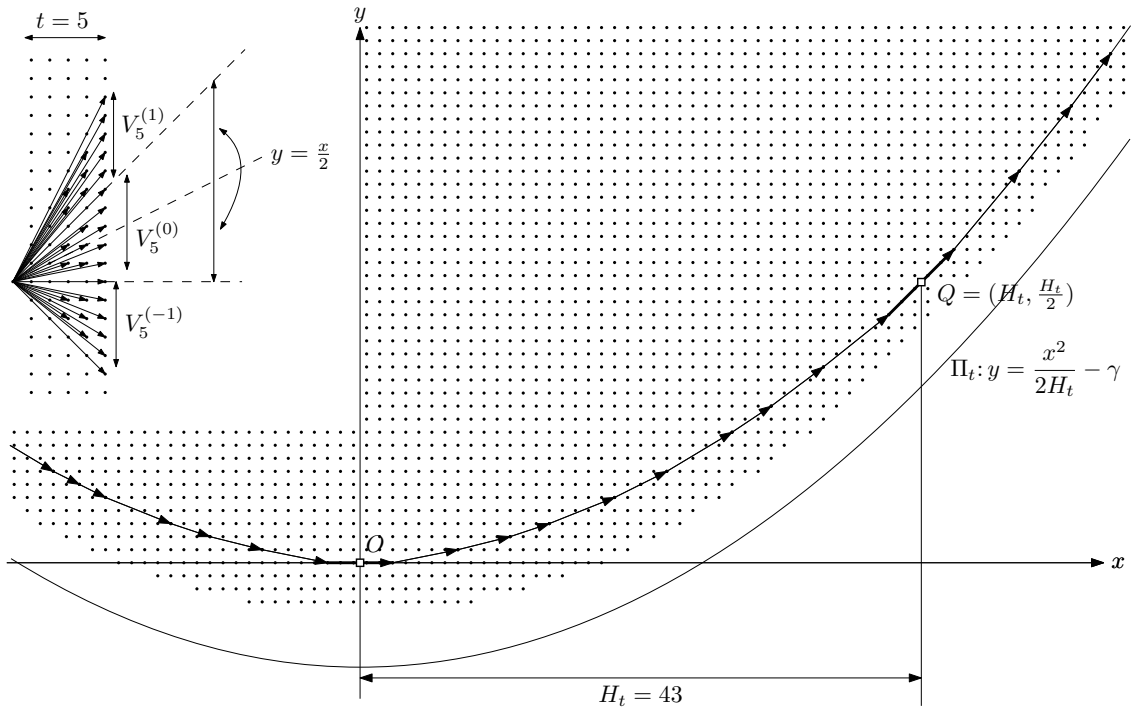

Figure 4: The grid parabola P_t for $t = 5$. The inset in the upper left corner shows some vectors of the set V_5, at a slightly enlarged scale. Π_t is the reference parabola defined by $y = \frac{x^2}{2H_t}$. Here it is shifted down by some offset γ.

edge of slope 0. This asymmetry is taken care of by including half of both edges in the vector from O to Q. Thus, the slope between O and Q averages out to $\frac{1}{2}$.

To see statement 2, note that the vectors that are matched in a pair sum to a vector with an even x-coordinate. The unmatched vectors in $V_t^{(0)}$ are the vector of slope $s = \frac{1}{2}$, which has an even x-coordinate, and the vector $\binom{t}{t}$, whose parity therefore decides the parity of H_t. □

2.1.1 Periodic continuation

The mapping $(x, y) \mapsto (x, y + ix)$ maps $V_t^{(0)}$ to $V_t^{(i)}$; hence it is sufficient to know $V_t^{(0)}$; all other sets $V_t^{(i)}$ are copies of $V_t^{(0)}$ where the slope of each vector is modified by an integer constant, leaving the x-coordinate fixed. This means that the continuation of P beyond the arc from O to Q is in some sense periodic: the same sequence of edges will appear again and again, only with modified slopes. The mapping $(x, y) \mapsto (x + H_t, y + H_t/2 + x)$ maps O to Q, and it maps the curve P to itself. The midpoints of the edges with integer slopes appear regularly at intervals of length H_t. The midpoint of the edge with slope i is $(iH_t, i^2H_t/2)$. These points lie on a parabola, which we call the *reference parabola*

$$\Pi_t \colon y = x^2/(2H_t),$$

and the polygonal chain P_t follows Π_t with bounded local deviations. We summarize these considerations in the following lemma, whose proof is straightforward.

Lemma 1. *The affine transformation*

$$\begin{pmatrix} x \\ y \end{pmatrix} \mapsto \begin{pmatrix} x + H_t \\ y + x + H_t/2 \end{pmatrix}$$

maps the grid to itself, and in addition, it maps both P_t and the reference parabola Π_t, or any vertical translate of it, to itself. □

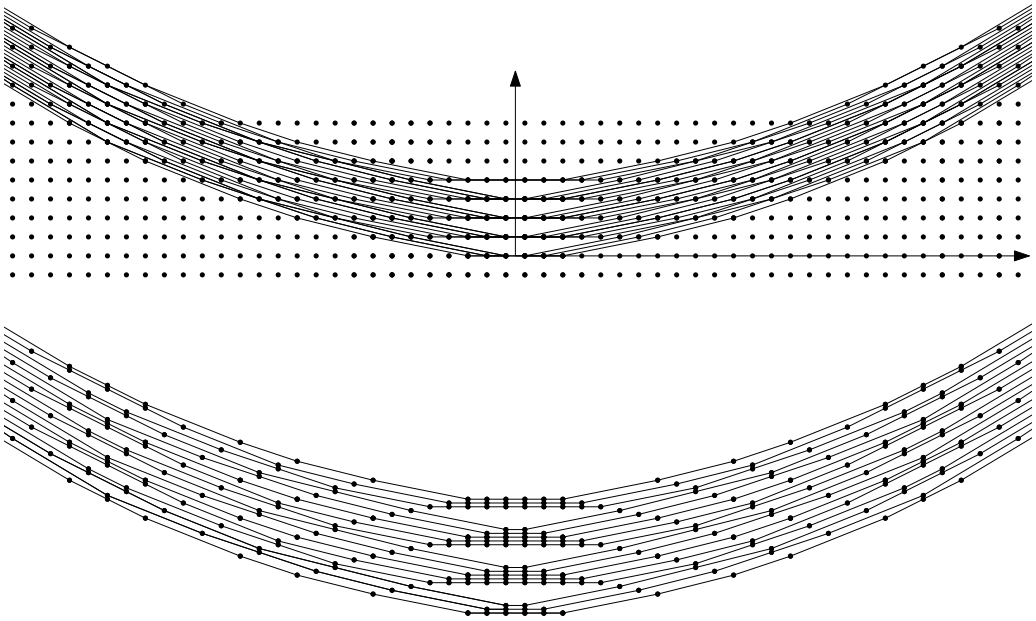

Figure 5: Consecutive peelings of P_5. Since consecutive peelings share many vertices, it is not easy to distinguish the curves. In the lower part, we have therefore vertically separated the consecutive peelings. This has the effect that some grid points appear in several copies with small vertical offsets, and horizontal grid lines get a curved appearance.

3 Grid peeling for parabolas

We start with the simple observation that grid peeling preserves inclusion:

Observation 1. *Let $U \subseteq U' \subset \mathbb{Z}^2$ be two sets of grid points that are* upward closed*: $(x, y) \in U \implies (x, y+1) \in U$. Let f denote one peeling step. Then $f(U) \subseteq f(U')$.* □

Observation 1 implies that if C and D are two convex x-monotone curves that extend from $x = -\infty$ to $x = +\infty$ (e.g. grid curve or an arbitrary smooth or piecewise smooth curve), and C lies everywhere (weakly) below D, then this relation is maintained by grid peeling.

Lemma 2. *P and Π advance at the same limiting speed.*

Proof. As already argued, P approximates Π in a global sense, while locally, there might be deviations. This implies that we can shift Π vertically down by some integer amount γ and ensure that the shifted parabola, denoted by $\Pi - \gamma$, lies completely below P. Figure 4 shows the parabola for $\gamma = 8$, but actually, $\gamma = 1$ should already be sufficient to push Π below P.

Now imagine that we start grid peeling simultaneously with P and with $\Pi - \gamma$, or more precisely, with the convex hull of the grid points on or above $\Pi - \gamma$. Applying the monotonicity property of Observation 1, we conclude that the evolution of $\Pi - \gamma$ always remains below the evolution of P. It can never overtake P, and in particular, the limiting speed of $\Pi - \gamma$, which is the same as the limiting speed of Π, is at most the limiting speed of P.

We can push Π upward and start with a parabola $\Pi + \gamma'$ that lies above P everywhere, and argue in the same way that the evolution of P can never overtake the evolution of $\Pi + \gamma'$, and thus, the limiting speed of Π is at least the limiting speed of P. □

3.1 Evaluating the horizontal period H_t

We have seen that H_t is the sum of the x-coordinates of the vectors in $V_t^{(0)}$. It is thus given by the following expression:

$$H_t = \sum_{(x,y)\in V_t^{(0)}} x = \sum_{\substack{0<y\le x\le t\\ \gcd(x,y)=1}} \left\lfloor \frac{t}{x} \right\rfloor x$$

This sequence appears in the Online Encyclopedia of Integer Sequences [12, A174405]. It starts with the values

$$H_1, H_2, \ldots = 1, 4, 11, 22, 43, 64, 107, 150, 211, 274, 385, 462, 619, 748, 895, 1066, 1339, \ldots$$

The sequence has been investigated by Sándor and Kramer [18], who showed the following asymptotic estimate:

Lemma 3.

$$H_t \sim \frac{2\zeta(3)}{\pi^2} t^3 \approx 0.243587656\, t^3$$

This can also be derived as a consequence of the more general Lemma 4, which is stated below. Section A gives several alternative expressions for H_t.

3.2 Distance between the grid parabola and the reference parabola

We want to analyze the deviation between the grid parabola and the reference parabola. While the reference parabola has an explicit expression, the grid parabola is given by a multistep process, as described in Section 2. For getting from the origin to an arbitrary vertex of P_t, we need to sum the vectors whose slope is at most some threshold α:

$$U_t^\alpha := \sum_{\substack{0\le x\le t\\ 0<y\le \alpha x\\ \gcd(x,y)=1}} \left\lfloor \frac{t}{x} \right\rfloor \binom{x}{y}$$

More precisely, since the sum includes only vectors with $y > 0$, it measures the distance from the right endpoint of the horizontal segment of P_t and not from the origin. Lemma 4, whose proof will be given in Appendix B, gives an asymptotic expression for this sum:

Lemma 4. *Let $0 \le \alpha \le 1$. Then*

$$U_t^\alpha = \frac{2\zeta(3)}{\pi^2} \binom{t^3\alpha + O(t^2 \log t)}{t^3\alpha^2/2 + O(t^2 \log t)}, \quad \textit{and} \quad H_t = \frac{2\zeta(3)}{\pi^2} t^3 + O(t^2 \log t).$$

The second expression is obtained from the first one by setting $\alpha = 1$ and looking only at the x-coordinate.

Proposition 2. *The vertical distance between the grid parabola P_t and the reference parabola Π_t is bounded by $O(t^2 \log t)$.*

Proof. By the periodic behavior of P_t and Π_t (Lemma 1), it suffices to look at the interval $0 \le x \le H_t$. Pick a point x_0 in this interval, see Figure 6. The corresponding point $\binom{x_0}{y_0}$ on Π_t has $y_0 = x_0^2/(2H_t)$, and the slope at this point is $\alpha := x_0/H_t \le 1$. As a first step, we find the point $\binom{x_1}{y_1}$ on P_t with the same slope α. We will show that it deviates from $\binom{x_0}{y_0}$ by at most $O(t^2 \log t)$ in each coordinate: By construction the grid parabola contains the vertex

$$\binom{x_1}{y_1} = \binom{t/2}{0} + U_t^\alpha.$$

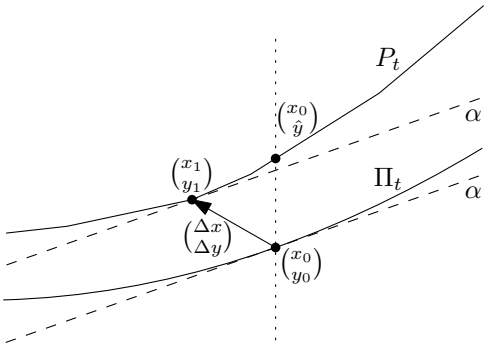

Figure 6: The vertical distance between P_t and Π_t

The correction term $t/2$ accounts for the fact that U_t^α does not include the vector $\binom{t}{0}$ and thus measures the distance from the right endpoint of the horizontal segment of P_t and not from the origin. Applying both parts of Lemma 4, we get

$$\begin{aligned}\binom{x_1}{y_1} = \binom{t/2}{0} + U_t^\alpha &= \frac{2\zeta(3)t^3}{\pi^2}\binom{\alpha}{\alpha^2/2} + \binom{O(t^2\log t)}{O(t^2\log t)} + \binom{t/2}{0} \\ &= \big(H_t + O(t^2\log t)\big)\binom{\alpha}{\alpha^2/2} + \binom{O(t^2\log t)}{O(t^2\log t)} \\ &= H_t\binom{\alpha}{\alpha^2/2} + \binom{O(t^2\log t)}{O(t^2\log t)} \\ &= \binom{x_0}{y_0} + \binom{\Delta x}{\Delta y}\end{aligned}$$

with $\Delta x, \Delta y = O(t^2\log t)$. In the range $0 \le x \le H_t$, the slope of P_t is bounded by 1. So when we move from x_1 to $x_0 = x_1 + \Delta x$ on P_t, we arrive at a point $(x_0, \hat{y})$ with $|\hat{y} - y_1| \le |\Delta x|$, and thus, the vertical distance $|\hat{y} - y_0|$ between P_t and Π_t is at most $|\Delta y| + |\Delta x| = O(t^2\log t)$. □

Figure 20 in Appendix E shows the actual difference $P_t - \Pi_t$ for a few selected values of t.

3.3 Comparison to true parabolas

Let $y = ax^2/2 + bx + c$. We are interested in the average (vertical) speed in which the curve moves upwards. If we start grid peeling with a parabola $y = ax^2 + bx + c$ for rational coefficients a and b, we can show that, after some irregular "preperiod", it will enter a periodic behavior: After a certain number Δm of steps, the same curve reappears, translated upward by Δy. We call Δm the *time period* and Δy the *vertical period* (to be distinguished from yet another period, the horizontal period H, which was introduced at the beginning). The *average (vertical) speed* is then $\Delta y/\Delta m$. However, if a or b is irrational, we no longer have a periodic behavior. For a more general curve, like $y = e^x$, different parts of the curve will move at different speeds, and a common average speed will not exist. For this reason, we define the *lower* and *upper* average speed.

Definition 1 (average speed)**.** Let C be the graph of a convex function on $\mathbb{R}$. We denote by $C + \gamma$ the copy of C vertically translated by γ (upwards for $\gamma > 0$, downwards for $\gamma < 0$).

For another such curve D, we write $C \le D$ if no point of C lies above D.

Let $f^{(m)}$ denote m steps of grid peeling.

The *lower average speed* $v_- = v_-(C)$ is defined as follows:

$$v_- = \liminf_{m\to\infty} \frac{\sup\{\,\gamma \mid C + \gamma \le f^{(m)}(C)\,\}}{m}$$

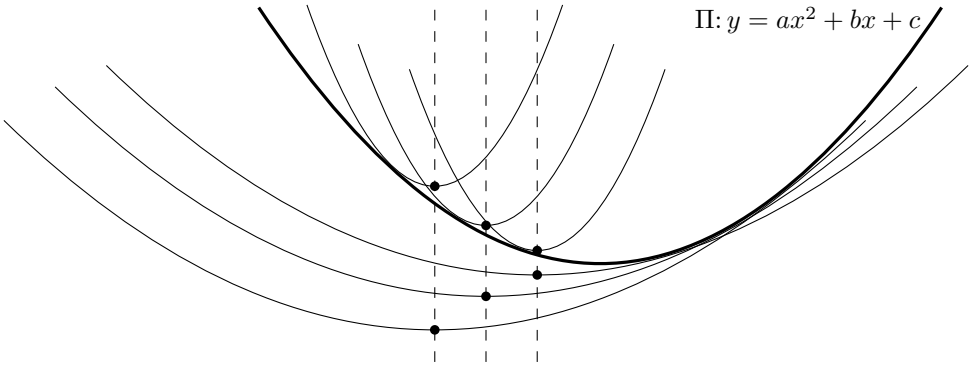

Figure 7: Upper and lower approximation of the parabola Π by "integer" parabolas

The *upper average speed* $v_+ = v_+(C)$ is defined similarly:

$$v_+ = \limsup_{m\to\infty} \frac{\inf\{\,\gamma \mid f^{(m)}(C) \le C + \gamma\,\}}{m}$$

If v_- and v_+ coincide, we call it simply the average speed $v = v(C)$.

We have the obvious inequalities $0 \le v_- \le v_+ \le \infty$. By approximating the parabola $y = ax^2/2 + bx + c$ from above and below by appropriate grid parabolas (see Figure 7), to which we apply Theorem 2, we arrive at the following result:

Theorem 3. *1. If $\frac{1}{H_t} < a < \frac{1}{H_{t-1}}$ and t is odd (or $a > \frac{1}{H_1} = 1$), then $v = 1/t$.*

2. If $\frac{1}{H_t} < a < \frac{1}{H_{t-1}}$ and t is even, then $\frac{1}{t+1} \le v_- \le v_+ \le \frac{1}{t-1}$.

3. If $a = \frac{1}{H_t}$ and t is odd, then $\frac{1}{t+2} \le v_- \le v_+ \le \frac{1}{t}$.

4. If $a = \frac{1}{H_t}$ and t is even, then $\frac{1}{t+1} \le v_- \le v_+ \le \frac{1}{t-1}$. □

The experiments in Section D suggest that the first statement also holds for even t, and for $a = \frac{1}{2H_t}$, v exists always and lies in the range $\frac{1}{t+1} \le v \le \frac{1}{t}$.

Proposition 3. *Let C be the graph of a convex function on $\mathbb{R}$. The upper and lower average speed is not changed by*

- *horizontal translation by an integer distance,*
- *or arbitrary vertical translation.*

Proof. It is clear that a translation by an integer vector does not change anything.

Consider an arbitrary vertical translation $C+\gamma$. Then (1) The integer translates $C_0 = C+\lfloor\gamma\rfloor$ and $C_1 = C + \lfloor\gamma\rfloor + 1$ have the same upper and lower average speeds as C, (2) they maintain a constant vertical distance of 1 during grid peeling, and (3) $C + \gamma$ is sandwiched between C_0 and C_1, and it maintains this relation during grid peeling. It follows that the upper and lower average speeds of C must agree with those of C_1 and C_2. □

One might be tempted to believe that a small horizontal translation should also not change the vertical speed. However, Section D.2 reports examples where translations cause the vertical speed to change, see Figure 15.

3.4 Refined grid peeling for parabolas, proof of Theorem 1

We prove our main theorem, Theorem 1 about the relation between grid peeling and ACSF for parabolas $y = ax^2/2 + bx + c$. We use (x, y) for the original coordinates, with a grid of spacing $1/n$, and $(\hat{x}, \hat{y}) = (nx, xy)$ for the scaled coordinates, with a unit grid. The curvature at the vertex of the parabola is a; thus the vertical speed of ACSF at this point (and thus everywhere, by affine invariance) is $a^{1/3}$.

At time T we have $y = ax^2/2+bx+c+Ta^{1/3}$, and $\hat{y} = \frac{a}{n}\hat{x}^2/2+b\hat{x}+cn+Tna^{1/3}$. Determine t such that $\frac{1}{H_t} \le \frac{a}{n} \le \frac{1}{H_{t-1}}$. So $\frac{a}{n} \approx \frac{1}{H_t}$ and Lemma 4 implies

$$\frac{n}{a} \approx H_t = \frac{2\zeta(3)t^3}{\pi^2} \cdot (1 + O(\log t/t)) = \Big(\frac{t}{c_{\mathrm{g}}}\Big)^3 \cdot (1 + O(\log t/t)),$$

which yields

$$t = c_{\mathrm{g}} \sqrt[3]{\frac{n}{a\big(1 + O(\log t/t)\big)}} + O(1) = c_{\mathrm{g}} \sqrt[3]{\tfrac{n}{a}} \cdot \big(1 + O(\log t/t)\big) = \Theta\Big(\sqrt[3]{\tfrac{n}{a}}\Big).$$

Here, the $O(1)$ term accounts for rounding t to an integer, and it also covers the uncertainty of Theorem 3, where t is sometimes replaced by $t-1$, $t+1$, or $t+2$. This additive error term is absorbed in the multiplicative error term $1 + O(\log t/t)$. By Theorem 3, the lower and upper average speed is

$$v \approx \frac{1}{t} = \frac{1}{c_{\mathrm{g}}} \sqrt[3]{\tfrac{a}{n}} \cdot \big(1 + O(\log t/t)\big)$$

After $m = \lfloor c_{\mathrm{g}} T n^{4/3} \rfloor$ steps, the vertical distance that the curve has moved up is therefore

$$mv + O(1) = Ta^{1/3}n\big(1 + O(\log t/t)\big) + O(1) = Ta^{1/3}n\big(1 + O(\sqrt[3]{\tfrac{a}{n}} \log \tfrac{n}{a})\big)$$

The difference to the movement of Π, which is $Tna^{1/3}$, is

$$O\big(Ta^{1/3}n \sqrt[3]{\tfrac{a}{n}} \log \tfrac{n}{a}\big) = O(Ta^{2/3}n^{2/3} \log \tfrac{n}{a}).$$

To this, we must add the distance between P_t and the reference parabola Π_t from Proposition 2, that is, $O(t^2 \log t) = O((\frac{n}{a})^{2/3} \log \frac{n}{a})$. Dividing by n, we conclude that the error term in terms of the original y-coordinates is

$$\big(O(Ta^{2/3}n^{2/3} \log \tfrac{n}{a}) + O((\tfrac{n}{a})^{2/3} \log \tfrac{n}{a})\big)/n = O\big((Ta^{2/3} + a^{-2/3})/n^{1/3} \log \tfrac{n}{a}\big). \quad \square$$

4 Proof of Theorem 2 about the period of the grid parabola

When we speak of *the curve*, we mean the grid parabola P_t after some iterations of peeling.

Let $s = a/b \in S_t$ be a fixed slope. We consider the supporting line g with slope s, and we study how it evolves during the peeling process, see Figure 8 for an illustration.

Definition 2. The *strip* of slope s is the vertical strip that bounds the segment of slope s in P_t. It goes from $x = L_s$ to $x = R_s$. We denote by $\ell = R_s - L_s$ the *width* of the strip.

The *extended strip* of slope s includes an additional margin of $\lfloor t/2 \rfloor$ on both sides. It goes from $\bar{L}_s = L_s - \lfloor t/2 \rfloor$ to $\bar{R}_s = R_s + \lfloor t/2 \rfloor$.

We state some obvious properties of the peeling process:

Observation 2. *Throughout the whole peeling process:*

(i) The supporting line g intersects the curve in a line segment, which might degenerate to a point.

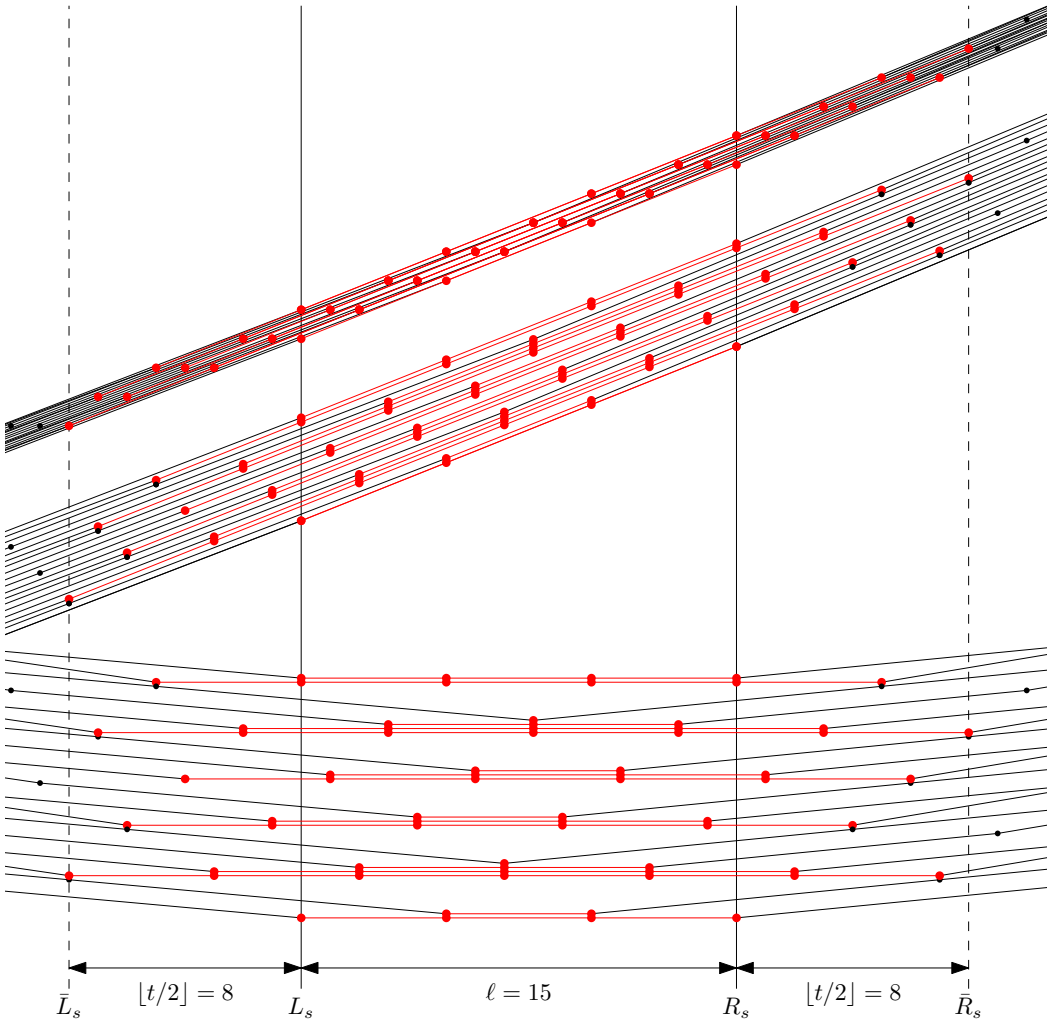

Figure 8: 17 consecutive iterations of the development of slope $s = 2/5$ for $t = 16$, starting with the curve P_t. The uppermost part shows the true situation. In the middle part, the successive curves are separated for better visibility, as in Figure 5. In the lowest part, an affine transformation has been applied to make the segment of interest horizontal; this allows the different slopes to be distinguished more easily. The segment of slope s is highlighted in red on each curve. The initial segment on P_{16} has horizontal length $\ell = \lfloor \frac{16}{5} \rfloor \times 5 = 15$. The region between the dashed lines is the extended strip.

(ii) If the segment contains $k \geq 1$ grid points, its horizontal length is $(k-1)b$.

(iii) At every peeling step, the two endpoints of this line segment or the single point is peeled.

(iv) As long as the segment contains at least 3 grid points, the supporting line does not change, and the number k of grid points on the segment decreases by 2. In this case, we say that the segment shrinks*.*

(v) If the segment contains only 1 or 2 grid points, the supporting line changes. We say that there is a jump *for slope s.* □

We use the following terminology: The *left endpoint of slope s* is the left endpoint of the segment of slope s; in case the segment degenerates to a single point, it is that point. In other words, it is the leftmost point where the supporting line of slope s touches the curve. The *right endpoint* is defined analogously. We will only deal with *horizontal* offsets, lengths, positions, and distances, and thus we will often omit the word *horizontal*.

In the following crucial lemma, Properties 1 and 2 predict *what* happens when a jump occurs. In particular, Property 2 characterizes the possible locations of the vertices after a jump. Property 3 describes the final position of the segment before the jump. This statement allows us to predict *when* a jump occurs. Property 3 can be easily worked out, *assuming* that the initial position after the previous jump satisfies Property 2. Properties 4 and 5 describe the situation when two consecutive slopes are involved.

Lemma 5. *The following properties hold throughout the peeling process:*

1. *(No grid line is skipped.) Whenever there is a jump, the supporting line g of slope s advances to the* next grid line *with slope s.*

2. *(The filling property.) After the supporting line g has advanced, the curve will contain precisely those grid points on g that lie within the extended strip of s. In other words, the segment fills the extended strip as much as possible. (See Figure 8 and 9.)*

3. *(Jump position) A jump of slope s occurs if and only if the left endpoint of slope s lies in the range*
$$L_s + \lfloor t/2 \rfloor - (b-1),\ \ldots,\ L_s + \lfloor t/2 \rfloor. \tag{4}$$
A symmetric property holds for the right endpoint.

4. *(There are no gaps.) For any two consecutive slopes $s = a/b$ and $s' = a'/b'$ from S_t, with $s < s'$, the right endpoint of slope s coincides with the left endpoint of slope s'. In particular, no edge has an intermediate slope between s and s'. This implies that only slopes from the set S_t appear in the curves.*

5. *(Breakpoint position) The breakpoint between two consecutive slopes s, s' is in the interval between $X - t/2$ and $X + t/2$, where $X = R_s = L_{s'}$ is the boundary between the corresponding strips. (See Figure 10.)*

Properties 1–3, which were discovered experimentally, are strong enough to predict the behavior of the supporting segment of slope s during the peeling process in a purely local manner, without looking at the whole curve. The proof that this is the evolution that actually takes place amounts to checking whether these local characterizations fit together when considering different slopes. In particular, we will look at two consecutive slopes (Properties 4 and 5). This will involve checking some cases, but with the rigid structure provided by the strong properties 1–3, one cannot really avoid to come up with the proof.

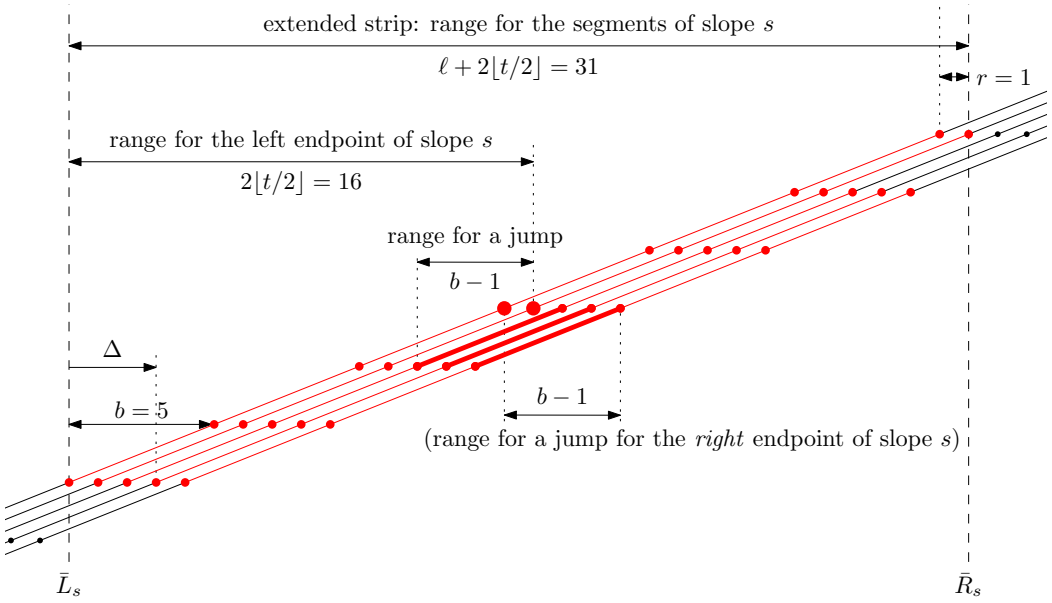

Figure 9: The $b = 5$ grid lines from Figure 8. $t = 16 = 3b + 1 = qb + r$. The initial segment on each line, immediately after the jump, is shown in red. The lines are considered according to the offset Δ of the leftmost grid point from the left edge of the extended strip. We have highlighted the last remaining single point or pair of points before the jump occurs.

Proof. We will show inductively that the claimed properties are maintained as invariants for all slopes throughout the peeling process.

We rely on the following properties of two consecutive slopes $s = \frac{a}{b}$ and $s' = \frac{a'}{b'}$, which follow from the definition of the slope set S_t (Section 2):

(I) The denominators b and b' are bounded by $b, b' \leq t$, and their sum is $b + b' > t$.

(Otherwise, the vector $\binom{b}{a} + \binom{b'}{a'}$ would give rise to a slope in S_t between s and s'.)

(II) The two vectors $\binom{b}{a}$ and $\binom{b'}{a'}$ form a lattice basis of the unit grid.

(Otherwise, they would span a parallelogram that contains interior points, and some of these points would lead to vectors with an intermediate slope between s and s' in S_t.)

As the basis for the induction, it can be seen without computation that the "original" segment of slope s of P_t falls in the pattern of analysis leading to Property 3: Indeed, it lies centrally in the extended strip. Thus, when extending it as much as possible within the extended strip and starting the peeling process, the starting segment will appear during this process, by symmetry. Also, the endpoints of consecutive segments match on P_t by construction, establishing Property 4 and Property 5 at the beginning.

For the induction step we consider two consecutive slopes s, s' and make sure that no matter if they make a jump or not, the properties of Lemma 5 hold. Thus we have four cases. In each case we prove properties 1,2, 4, 5, and then assuming properties 1,2, 4, 5, we prove Property 3 all at once.

Case 1: s and s' both shrink: We show that this is not possible. Assume that s, s' both shrink. Since no jump occurs for s', by Property 3 the rightmost possible position of the left endpoint of s' is $L_{s'} + \lfloor t/2 \rfloor - b'$. Symmetrically, the leftmost possible position of the right endpoint of s is $R_s - \lfloor t/2 \rfloor + b$, and therefore $R_s - \lfloor t/2 \rfloor + b \leq L_{s'} + \lfloor t/2 \rfloor - b'$. Since $L_{s'} = R_s$, it follows that $-\lfloor t/2 \rfloor + b \leq \lfloor t/2 \rfloor - b'$, or $b + b' \leq 2\lfloor t/2 \rfloor \leq t$, which contradicts (I).

Case 2: s jumps and s' shrinks: We claim that the endpoint of the shrunken segment for s' arrives at the next grid line with slope s, and its position on this line matches the position

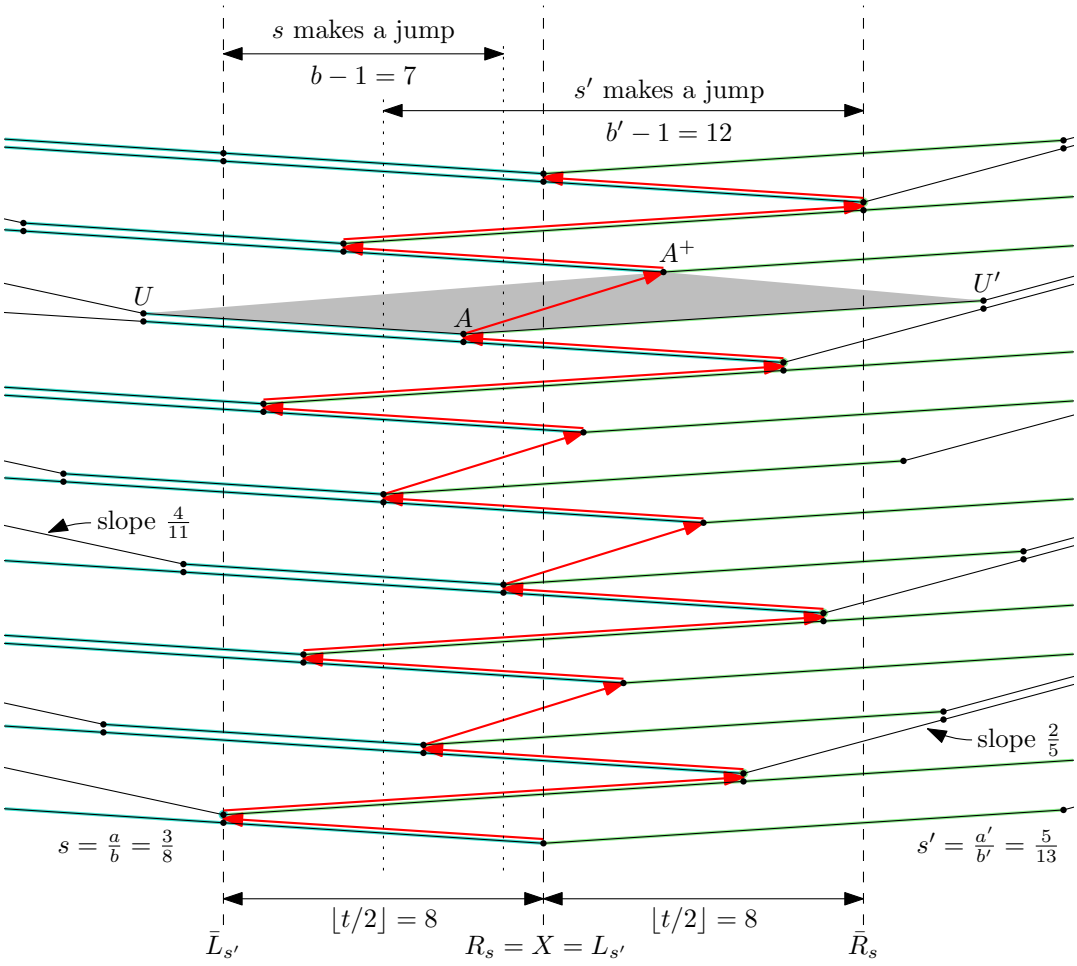

Figure 10: The transition between slope $s = 3/8$, with vector $\binom{16}{6} \in V_t$, and $s' = 5/13$, with vector $\binom{13}{5} \in V_t$, for $t = 16$. The figure is drawn after an affine transformation, following the conventions of the lower part of Figure 8. The right endpoint of slope s always coincides with the left endpoint of slope s', and it varies in the interval between $X - \lfloor t/2 \rfloor$ and $X + \lfloor t/2 \rfloor$.

for the right endpoint of s predicted by Property 2. The left endpoint of s' moves by the vector $\binom{b'}{a'}$, and since $\binom{b'}{a'}$ and $\binom{b}{a}$ form a lattice basis (II), the supporting line of slope s will indeed jump to the next grid line of slope s, establishing Property 1 in this case.

We claim that this new left endpoint of s' is indeed the rightmost grid point on this line in the extended strip for s (establishing Property 2). We show that it lies in the extended strip of s, but the point *after* this point on the grid line of slope s is already outside the extended strip.

To show the former, consider the rightmost possible position for the left endpoint of s' before shrinking. It is $L_{s'} + \lfloor t/2 \rfloor - b'$ by Property 3. After shrinking, it is $L_{s'} + \lfloor t/2 \rfloor = R_s + \lfloor t/2 \rfloor = \bar{R}_s$, and thus it lies in the extended strip of s. To show the latter, consider the leftmost possible position for the left endpoint of s' before shrinking. It is $\bar{L}_{s'} = X - \lfloor t/2 \rfloor$ by Property 3. After shrinking, it is $X - \lfloor t/2 \rfloor + b'$. The point after this point is at offset b, and $X - \lfloor t/2 \rfloor + b' + b > X - \lfloor t/2 \rfloor + t \geq X + \lfloor t/2 \rfloor = \bar{R}_s$, by (I), and thus this point is already outside the extended strip.

Therefore, the new left endpoint of s' coincides with the new right endpoint of s, establishing Property 4 and Property 5 in this case.

Case 3: s shrinks and s' jumps: The situation is symmetric to Case 2.

Case 4: s and s' both jump: By Property 3 the position x of the breakpoint $A = \binom{x}{y}$

before the jump is in the interval

$$X + \lfloor t/2 \rfloor - b' < x < X - \lfloor t/2 \rfloor + b \tag{5}$$

Let U be the previous point on the grid line of slope s through A, and let U' be the next point on the grid line of slope s' through A. Construct the parallelogram $UAU'A^+$. Such a parallelogram is shaded in Figure 10. We know that both supporting lines of slope s and s' must advance at least to the next grid line. Those two grid lines intersect at the fourth point $A^+ = \binom{x^+}{y^+}$ of this parallelogram with $x^+ = x - b + b'$. We will show two things:

(a) The point A^+ is not peeled until after the jump. Thus it will be the common right endpoint of slope s and left endpoint of slope s'.

(b) It is indeed the rightmost grid point on the grid line of slope s in the extended strip of s. (Symmetrically, it is the leftmost point on the grid line in the extended strip of s'.)

To prove (a), assume w.l.o.g. that $b \le b'$, so that the segment AU' lies below A^+. We are done if we show that this segment is part of the boundary when A is peeled. Assume otherwise. Then A would be not only the left endpoint of slope s', but also the right endpoint of slope s' when it is peeled. According to Property 3, this means that $x \ge R_{s'} - \lfloor t/2 \rfloor$. Let $\ell_{s'} \ge b'$ denote the length of the strip of slope s'. Then, with $b \le b' \le \ell_{s'}$ we get a contradiction to (5):

$$x \ge R_{s'} - \lfloor t/2 \rfloor \ge R_{s'} - \ell_{s'} - \lfloor t/2 \rfloor + b = X - \lfloor t/2 \rfloor + b > x$$

To prove (b), note that A^+ lies in the extended strip for s because $x^+ = x - b + b' < X - \lfloor t/2 \rfloor + b' \le X - \lfloor t/2 \rfloor + t$, by the right inequality of (5), and hence $x^+ \le X + \lfloor t/2 \rfloor$. On the other hand, the next grid point on the line of slope s has x-coordinate $x^+ + b = x + b' > X + \lfloor t/2 \rfloor$, by the left inequality of (5), and this is outside the extended strip for s.

Now that we have established the first four invariants in all cases, we prove Property 3, assuming Property 2 has been true so far.

Let $t = qb + r$, with $0 \le r < b$. Then $qb = \ell$ is the (horizontal) length of the vector in V_t that forms the segment of slope s on P_t. We have defined it as the width of the strip.

To illustrate Property 2, Figure 9 shows the possible cases how the segment of slope s can lie on the grid line, immediately after a jump occurs, according to this property. On every grid line, the grid points form an arithmetic progression with (horizontal) increment b. The different grid lines are distinguished by the offset Δ of the leftmost grid point from the left edge of the extended strip. There are b possibilities, $0 \le \Delta < b$.

For the sake of the following analysis, we have sorted the lines by Δ in Figure 9. (This is not the order in which they occur from bottom to top. The true order in this example is $\Delta = 0, 2, 4, 1, 3, 0, \ldots$, see Figure 8.)

For simplicity, we focus on the case when t is even [and put the odd case into brackets].

Let us start with the case $\Delta = 0$ (the topmost line in Figure 9). In a strip of width t, we can fit q segments of length b, with $q + 1$ points, leaving a remainder of length r. The extended strip has width $t + \ell$ [$t - 1 + \ell$]. Since the extra length ℓ is filled precisely by q segments, we can fit q additional segments of length b, for a total of $2q + 1$ points. [For odd t, the last claim holds only when $r > 0$.]

Since the number of points is odd, the last peeled segment on this line before the jump is a singleton, after q steps and at distance $qb = \ell$ from the left boundary $\bar{L}_s$ of the extended strip, or distance $\ell - \lfloor t/2 \rfloor$ from L_s.

We can increase Δ up to r [$r - 1$] without changing the situation:

- For $\Delta = 0, 1, \ldots, r$ $[\Delta = 0, 1, \ldots, r-1]$, the number k of points is odd, and for the last point that is peeled, the distance from L_s is in the range

$$\ell - t/2, \ldots, \ell - t/2 + r \quad [\ell - \lfloor t/2 \rfloor, \ldots, \ell - \lfloor t/2 \rfloor + r - 1].$$

  Since $\ell + r = t$, this range simplifies to $\ell - \lfloor t/2 \rfloor, \ldots, \lfloor t/2 \rfloor$.

Starting from $\Delta = r + 1$ $[\Delta = r]$, the situation changes. We have now an even number $2q$ of points, and the last peeled segment is a proper segment with a *pair* of points. The left peeled point is at distance $\Delta + (q-1)b = \Delta + \ell - b$ from $\bar{L}_s$, or at an offset $\Delta + \ell - b - \lfloor t/2 \rfloor$ from L_s (This offset may be negative, in which case it denotes an offset to the left.)

- For $\Delta = r + 1, \ldots, b - 1$ $[\Delta = r, \ldots, b - 1]$, the number k of points is even, and for left point of the last peeled pair, the distance from L_s is in the range

$$r + 1 + \ell - b - t/2, \ldots, b - 1 + \ell - b - t/2 \quad [r + \ell - b - \lfloor t/2 \rfloor, \ldots, b - 1 + \ell - b - \lfloor t/2 \rfloor].$$

  Since $\ell + r = t$, this range simplifies to $\lfloor t/2 \rfloor - b - 1, \ldots, \ell - \lfloor t/2 \rfloor - 1$.

Combining the ranges for two cases establishes Property 3, and this concludes the proof of Lemma 5. □

Proposition 4. *The left endpoint of slope s is at distance at most $\lfloor t/2 \rfloor$ from L_s (on the left or on the right), see Figure 9. Every position in this range occurs.*

Proof. Property 3 describes b possibilities before a jump, one value for each of the b residue classes modulo b, and Property 2 suggests b possibilities after a jump, namely $\Delta = 0, 1, \ldots, b-1$. Since for every Δ, the jump must occur at *some* point, the range (4) uniquely characterizes this point.

By Property 3, the left endpoint of slope s can never deviate more than $\lfloor t/2 \rfloor$ from L_s to the right, and by Property 2, it cannot deviate more than $\lfloor t/2 \rfloor$ from L_s to the left. Thus, the left endpoint of slope s is at distance at most $\lfloor t/2 \rfloor$ from L_s. In fact, since there is a grid line of slope s passing through every such point, and no grid line is skipped (Property 1), every point in this range will be peeled once as the left endpoint of slope s. □

There are $2\lfloor t/2 \rfloor + 1$ different offsets at distance at most $\lfloor t/2 \rfloor$ from L_s, and exactly one of them is always peeled. Therefore, after $2\lfloor t/2 \rfloor + 1$ steps the same segment of slope s repeats, one unit higher. This is true for any slope, so after $2\lfloor t/2 \rfloor + 1$ steps the same chain repeats one unit higher. It means the peeling process is periodic with period $2\lfloor t/2 \rfloor + 1$, and this concludes the proof of Theorem 2. □

5 Future research

The obvious open problem is to prove the relation between grid peeling and the ACSF for arbitrary convex curves. As a first challenge, one might try the case of a circle. The natural approach is to leverage Theorem 1 by locally approximating the curve by parabolas.

Some of the phenomena that were revealed by the experiments described in Section D are still awaiting an explanation.

References

[1] Luis Alvarez, Frédéric Guichard, Pierre-Luis Lions, and Jean-Michel Morel. Axioms and fundamental equations of image processing. *Arch. Rational Mech. Anal.*, 123:199–257, 1993. doi:10.1007/BF00375127.

[2] Sergey Avvakumov and Gabriel Nivasch. Homotopic curve shortening and the affine curve-shortening flow. *Journal of Computational Geometry*, 12:145–177, 2021. doi:10.20382/jocg.v12i1a7.

[3] Imre Bárány, Matthieu Fradelizi, Xavier Goaoc, Alfredo Hubard, and Günter Rote. Random polytopes and the wet part for arbitrary probability distributions. *Annales Henri Lebesgue*, 3:701–715, 2020. arXiv:1902.06519, doi:10.5802/ahl.44.

[4] Imre Bárány and David G. Larman. Convex bodies, economic cap coverings, random polytopes. *Mathematika*, 35:274–291, 1988. doi:10.1112/S0025579300015266.

[5] Imre Bárány and Norihide Tokushige. The minimum area of convex lattice n-gons. *Combinatorica*, 24(11):171–185, 2004. doi:10.1007/s00493-004-0012-0.

[6] Jeff Calder and Charles K. Smart. The limit shape of convex hull peeling. *Duke Mathematical Journal*, 169(11):2079–2124, 2020. arXiv:1805.08278, doi:10.1215/00127094-2020-0013.

[7] Frédéric Cao. *Geometric Curve Evolution and Image Processing*, volume 1805 of *Lecture Notes in Mathematics*. Springer, Berlin, Heidelberg, 2003. doi:10.1007/b10404.

[8] Travis Dillon and Narmada Varadarajan. Explicit bounds for the layer number of the grid, 2023. arXiv:2302.04244.

[9] David Eppstein, Sariel Har-Peled, and Gabriel Nivasch. Grid peeling and the affine curve-shortening flow. *Experimental Mathematics*, 29(3):306–316, 2020. arXiv:1710.03960, doi:10.1080/10586458.2018.1466379.

[10] Sariel Har-Peled and Bernard Lidický. Peeling the grid. *SIAM Journal on Discrete Mathematics*, 27(2):650–655, 2013. arXiv:1302.3200, doi:10.1137/120892660.

[11] G. H. Hardy and E. M. Wright. *An Introduction to the Theory of Numbers*. Oxford Science Publications, 1979.

[12] The On-Line Encyclopedia of Integer Sequences. URL: http://oeis.org/.

[13] Ch. Radoux. Note sur le comportement asymptotique de l'indicateur d'Euler. *Ann. Sci. Bruxelles, Ser. I*, 91:13–18, 1977.

[14] Marko Riedel. Answer to *Euler phi function, number theory*. Mathematics Stack Exchange, 2014. version: 2014-05-08. URL: https://math.stackexchange.com/q/787082.

[15] Moritz Rüber. Die Gitterschälung und der affine Kurvenfluss auf Parabeln. M. Ed. thesis, Freie Universität Berlin, Department of Computer Science, November 2021.

[16] Guillermo Sapiro and Allen Tannenbaum. Affine invariant scale-space. *Int. J. Comput. Vision*, 11:25–44, 1993. doi:10.1007/bf01420591.

[17] Guillermo Sapiro and Allen Tannenbaum. On affine plane curve evolution. *Journal of Functional Analysis*, 119(1):79–120, 1994. doi:10.1006/jfan.1994.1004.

[18] J. Sándor and A. V. Kramer. Über eine zahlentheoretische Funktion. *Mathematica Moravica*, 3:53–62, 1999. URL: http://www.moravica.ftn.kg.ac.rs/Vol_3/10-Sandor-Kramer.pdf.

A Alternative expressions for the horizontal period H_t

The following long chain of equations and estimates, which we will discuss step by step, includes several different expressions for the quantity H_t. We denote by $\mathbb{P} = \{\, (i,j) \in \mathbb{Z} \times \mathbb{Z} \mid \gcd(i,j) = 1 \,\}$ the set of *primitive vectors*.

$$H_t := \sum_{\substack{0<y\le x\le t \\ (x,y)\in\mathbb{P}}} \left\lfloor \frac{t}{x} \right\rfloor x \tag{6}$$

$$= \sum_{1\le x\le t} \sum_{\substack{0<y\le x \\ (x,y)\in\mathbb{P}}} \left\lfloor \frac{t}{x} \right\rfloor x = \sum_{1\le x\le t} \phi(x) \left\lfloor \frac{t}{x} \right\rfloor x \tag{7}$$

$$= \sum_{1\le j\le i\le t} \frac{i}{\gcd(i,j)} \tag{8}$$

$$= \sum_{1\le i\le t} \sum_{1\le j\le i} \frac{i}{\gcd(i,j)} \tag{9}$$

$$= \sum_{1\le i\le t} \sum_{d\mid i} d\phi(d) \tag{10}$$

$$= \frac{2\zeta(3)}{\pi^2} t^3 + O(t^2 \log t) \tag{11}$$

$$\sim \frac{2\zeta(3)}{\pi^2} t^3 \tag{12}$$

After partitioning the double sum over x and y into two nested sums, the last expression in (7) expresses the inner sum, in which the summation variable y does not appear in the summand, in terms Euler's totient function $\phi(x)$, the number of residue classes y modulo x that are relatively prime to x.

The asymptotic expression (12) is due to Sándor and Kramer [18]. They define the function that they investigate by the expression (9), using the notation $\psi_1(i)$ for the inner sum in (9), and they establish equality between (9) and the last expression in (7) [18, §6, formula (13) with $\alpha = 1$. Formula (13‴), which should apply here, has an obvious typo]. The expressions (8) and (9) are obviously equivalent. We indicate why (8) is equal to (6), thus establishing equality of all expressions (6–9):

In the sum (6), only primitive vectors appear, but every primitive vector $(x,y) \in \mathbb{P}$ is taken with multiplicity $\lfloor t/x \rfloor$. If we look at the multiples $(i,j) = (kx, ky)$ of each primitive vector (x,y) for $k = 1, 2, \ldots, \lfloor t/x \rfloor$, we get *all* integer vectors in the triangle $0 < j \le i \le t$. In the sum (8), each vector (i,j) contributes the x-coordinate of the primitive vector $(x,y) = (i/k, j/k)$, since $k = \gcd(x,y)$. Thus, in total, the vector (x,y) is taken $\lfloor t/x \rfloor$ times in (8), and we get the same sum.

Formula (10) follows from (9) by splitting the integers $j = 1, \ldots i$ according to the value of $i/\gcd(i,j) = d$, cf. [18, §2, formula (1)].

The asymptotic expression (12) is given in [18, equation (23), p. 61]. A different proof, using the Wiener-Ikehara Theorem, was sketched by Marko Riedel on Mathematics Stack Exchange [14]. The slightly stronger statement (11) with the explicit error term follows from Lemma 4.

B Proof of Lemma 4 about the points on the grid parabola

The proof follows standard ideas; in particular, it uses an easy adaptation of the arguments that were used for the special case $\alpha = 1$ [18], as stated in Lemma 4. Following [18, p. 61], we reduce

the computation of U_t^α to the estimation of the vector $R^\alpha(u)$, which is defined as follows for any real parameter u:

$$R^\alpha(u) := \sum_{\substack{1\le x\le u\\ 0<y\le \alpha x\\ (x,y)\in\mathbb{P}}} \binom{x}{y} \tag{13}$$

We start from the definition of U_t^α and regroup and reformulate sums:

$$\begin{aligned} U_t^\alpha &= \sum_{\substack{1\le x\le t\\ 0<y\le \alpha x\\ (x,y)\in\mathbb{P}}} \left\lfloor \frac{t}{x} \right\rfloor \binom{x}{y} \\ &= \sum_{\substack{1\le x\le t\\ 0<y\le \alpha x\\ (x,y)\in\mathbb{P}}} \sum_{\substack{k\ge 1\\ xk\le t}} \binom{x}{y} = \sum_{k\ge 1} \sum_{\substack{1\le x\le t\\ xk\le t\\ 0<y\le \alpha x\\ (x,y)\in\mathbb{P}}} \binom{x}{y} = \sum_{k\ge 1} \sum_{\substack{1\le x\le t/k\\ 0<y\le \alpha x\\ (x,y)\in\mathbb{P}}} x \\ &= \sum_{k\ge 1} R^\alpha(\tfrac{t}{k}) \end{aligned} \tag{14}$$

For $R^\alpha(u)$, we will use the following asymptotic estimate, whose proof is given below:

Lemma 6. *For $0 \le \alpha \le 1$,*

$$R^\alpha(u) = \frac{2}{\pi^2} \begin{pmatrix} u^3\alpha + O(u^2 \log u) \\ u^3\alpha^2/2 + O(u^2 \log u) \end{pmatrix} \tag{15}$$

as $u \to \infty$.

Substitution of (15) in (14) gives our claimed asymptotic formula for U_t^α:

$$\begin{aligned} U_t^\alpha = \sum_{k\ge 1} R^\alpha\big(\tfrac{t}{k}\big) &= \sum_{k\ge 1} \frac{2}{\pi^2 k^3} \begin{pmatrix} t^3\alpha \\ t^3\alpha^2/2 \end{pmatrix} + \sum_{k\ge 1} \begin{pmatrix} O\big(\frac{t^2}{k^2}\log\frac{t}{k}\big) \\ O\big(\frac{t^2}{k^2}\log\frac{t}{k}\big) \end{pmatrix} \\ &= \frac{2\zeta(3)}{\pi^2} \begin{pmatrix} t^3\alpha \\ t^3\alpha^2/2 \end{pmatrix} + \begin{pmatrix} O(t^2\log t) \\ O(t^2\log t) \end{pmatrix} \end{aligned}$$

Proof of Lemma 6. We mention that the special case $\alpha = 1$ and the x-coordinate of $R^1(u)$ is given (without the error bound) in Sándor and Kramer [18, p. 61, (20)]:

$$\sum_{\substack{1\le y\le x\le u\\ (x,y)\in\mathbb{P}}} x = \sum_{1\le x\le u} \sum_{\substack{1\le y\le x\\ (x,y)\in\mathbb{P}}} x = \sum_{1\le x\le u} x\phi(x) \sim \frac{2u^3}{\pi^2}$$

There, this asymptotic expression is derived as an easy consequence of a general statement of Radoux [13] about the sum $\sum_{x=1}^u f(\frac{x}{u})\phi(x)$ being asymptotically equal to $6u^2/\pi^2 \int_{z=0}^1 zf(z)\,dz$ for an arbitrary function f, provided that $zf(z)$ is continuous. (The deeper reason behind this statement is that the fraction of primitive vectors among the integer vectors in *any* sufficiently large "well-behaved" region is $1/\zeta(2)$. Examples of well-behaved regions for which this statement holds are convex regions with a limit on the ratio between incircle and circumcircle, or dilates of a fixed convex region.)

The following proof of Lemma 6 adapts the textbook derivation of the similar formula

$$\sum_{\substack{1\le y\le x\le u\\ (x,y)\in\mathbb{P}}} 1 = \sum_{x=1}^{\lfloor u\rfloor} \phi(x) = \frac{u^2}{2\zeta(2)} + O(u\log u) \sim \frac{3u^2}{\pi^2}$$

in [11, Theorem 330], a result that goes back to Mertens in 1874.

We use the notation $T^\alpha(u)$ for the sum (13) without the condition that (x, y) should be primitive:

$$T^\alpha(u) := \sum_{\substack{1\le x\le u\\ 1\le y\le \alpha x}} \binom{x}{y} \tag{16}$$

$$= \sum_{x=1}^{\lfloor u\rfloor} \binom{x\lfloor \alpha x\rfloor}{\lfloor \alpha x\rfloor(\lfloor \alpha x\rfloor+1)/2} \tag{17}$$

$$= \sum_{x=1}^{\lfloor u\rfloor} \binom{\alpha x^2+O(x)}{\alpha^2 x^2/2+O(x)} \tag{18}$$

$$= \binom{\alpha}{\alpha^2/2}\left(\frac{\lfloor u\rfloor^3}{3}+\frac{\lfloor u\rfloor^2}{2}+\frac{\lfloor u\rfloor}{6}\right)+\binom{O(u^2)}{O(u^2)} \tag{19}$$

$$= \binom{\alpha}{\alpha^2/2}\frac{u^3}{3}+\binom{O(u^2)}{O(u^2)} \tag{20}$$

We claim that the $O(u^2)$ error terms in (20) can be explicitly bounded by

$$\left\| T^\alpha(u) - \binom{\alpha}{\alpha^2/2}\frac{u^3}{3}\right\|_\infty \le E(u) := \begin{cases} \frac{u^3}{3} & \text{for } 0\le u<1\\ \frac{5u^2}{3} & \text{for } u\ge 1\end{cases} \tag{21}$$

The bound for the first case, $u < 1$, is trivial because $T^\alpha(u) = \binom{0}{0}$ in this case. For the second case, $u \ge 1$, we accumulate the error bounds for the successive steps of the above derivation. The $O(x)$ error term in the transition from (17) to (18) is bounded (in absolute value) by x in the first coordinate and by $\alpha x/2 \le x$ in the second coordinate. Thus, we can bound each of the $O(u^2)$ terms in (19) by $u(u+1)/2 \le u(2u)/2 = u^2$.

The change in the factor between the term $A(u) := \frac{\lfloor u\rfloor^3}{3}+\frac{\lfloor u\rfloor^2}{2}+\frac{\lfloor u\rfloor}{6}$ in (19) and the factor $u^3/3$ in (20) is bounded by $2u^2/3$, as can be checked by an easy computation:

$$A(u) = \tfrac{\lfloor u\rfloor^3}{3}+\tfrac{\lfloor u\rfloor^2}{2}+\tfrac{\lfloor u\rfloor}{6} \le \tfrac{u^3}{3}+\tfrac{u^2}{2}+\tfrac{u}{6} \le \tfrac{u^3}{3}+\tfrac{u^2}{2}+\tfrac{u^2}{6}$$
$$A(u) = \tfrac{\lfloor u\rfloor^3}{3}+\tfrac{\lfloor u\rfloor^2}{2}+\tfrac{\lfloor u\rfloor}{6} \ge \tfrac{(u-1)^3}{3}+\tfrac{(u-1)^2}{2}+\tfrac{u-1}{6} = \tfrac{u^3}{3}-\tfrac{u^2}{2}+\tfrac{u}{6} \ge \tfrac{u^3}{3}-\tfrac{u^2}{2}-\tfrac{u^2}{6}.$$

and therefore, $|A(u)-\frac{u^3}{3}| \le \frac{2u^2}{3}$. Adding the two contributions together gives the claimed bound of $u^2 + 2u^2/3 = 5u^2/3$.

Comparing (13) with the sum (16), for which we have an explicit formula, we want to exclude the vectors (x, y) that are not primitive, i.e., where both x and y are multiples of one of the primes $2, 3, 5, 7, 11, \ldots$. By the inclusion-exclusion formula, we have to subtract the contribution of those vectors that are divisible by 2, by 3, by 5, etc., add the vectors that are divisible by *two* primes, subtract the vectors that are divisible by three primes, etc. The contribution of the vectors that are divisible by n is $nT^\alpha(\frac{u}{n})$, as these vectors are all integer vectors from the smaller region $0 < x \le u/n$, $0 \le y \le \alpha x$, scaled by n. We obtain:

$$\begin{aligned} R^\alpha(u) &= T^\alpha(u) - \left(2T^\alpha(\tfrac{u}{2})+3T^\alpha(\tfrac{u}{3})+5T^\alpha(\tfrac{u}{5})+\cdots\right)\\ &\quad + \left(2\cdot 3\cdot T^\alpha(\tfrac{u}{2\cdot 3})+2\cdot 5\cdot T^\alpha(\tfrac{u}{2\cdot 5})+\cdots\right)\\ &\quad - \left(2\cdot 3\cdot 5\cdot T^\alpha(\tfrac{u}{2\cdot 3\cdot 5})+\cdots\right)+\cdots\\ &= \sum_{n=1}^{\infty}\mu(n)nT^\alpha(\tfrac{u}{n}), \end{aligned}$$

In the last line, we have expressed the alternating sum in terms of the Möbius function

$$\mu(n) = \begin{cases} +1, & \text{if } n \text{ is the product of an even number of distinct primes,} \\ -1, & \text{if } n \text{ is the product of an odd number of distinct primes,} \\ 0, & \text{otherwise, i.e., if } n \text{ is not square-free.} \end{cases}$$

We now use the approximation (20) for $T^\alpha(\frac{u}{n})$

$$R^\alpha(u) = \sum_{n=1}^{\infty} \mu(n) n T^\alpha(\tfrac{u}{n}) = \sum_{n=1}^{\infty} \mu(n) \frac{u^3}{3n^2} \binom{\alpha}{\alpha^2/2} + E_0 \tag{22}$$

and bound the error E_0 by (21):

$$\begin{aligned} \|E_0\|_\infty &\le \sum_{n=1}^{\infty} \left|\mu(n) n E(\tfrac{u}{n})\right| \le \sum_{n=1}^{\infty} n E(\tfrac{u}{n}) \\ &\le \sum_{n=1}^{\lfloor u \rfloor} \frac{5u^2}{3n} + \sum_{n=\lfloor u \rfloor+1}^{\infty} \frac{u^3}{3n^2} = \frac{5u^2}{3} \cdot O(\log u) + \frac{u^3}{3} \cdot O(\tfrac{1}{u}) = O(u^2 \log u) \end{aligned}$$

The first term in (22) can be expressed in terms of the zeta-function using the well-known relation [11, Theorem 287] (which also derives from the inclusion-exclusion formula)

$$\begin{aligned} \sum_{n=1}^{\infty} \frac{\mu(n)}{n^2} &= \left(1 - \frac{1}{2^2}\right)\left(1 - \frac{1}{3^2}\right)\left(1 - \frac{1}{5^2}\right)\left(1 - \frac{1}{7^2}\right)\cdots \\ &= \frac{1}{1+\frac{1}{2^2}+\frac{1}{4^2}+\frac{1}{8^2}+\cdots} \cdot \frac{1}{1+\frac{1}{3^2}+\frac{1}{9^2}+\frac{1}{27^2}+\cdots} \cdot \frac{1}{1+\frac{1}{5^2}+\frac{1}{25^2}+\frac{1}{125^2}+\cdots}\cdots \\ &= \frac{1}{\sum_{n=1}^{\infty} \frac{1}{n^2}} = \frac{1}{\zeta(2)} = \frac{6}{\pi^2}. \end{aligned}$$

We obtain

$$R^\alpha(u) = \sum_{n=1}^{\infty} \mu(n) \frac{u^3}{3n^2} \binom{\alpha}{\alpha^2/2} + E_0 = \frac{6u^3}{3\pi^2} \binom{\alpha}{\alpha^2/2} + E_0 = \frac{2}{\pi^2} \binom{u^3\alpha + O(u^2 \log u)}{u^3\alpha^2/2 + O(u^2 \log u)}. \quad \square$$

C Minimum-area convex lattice polygons and grid parabolas

Our grid parabolas P_t make their appearance in a different context: the convex lattice n-gons of minimum area for a given number n of vertices, see Figure 11 for an example. Bárány and Tokushige [5] showed that, as n increases, the smallest n-gon resembles a more and more oblong ellipse-like shape, whose "axes" grow like n^2 and n, respectively, see the schematic drawing in Figure 12. It follows from their analysis (but it is not stated) that, after a unimodular transformation, the optimal n-gons are composed of pieces of the grid parabolas $P_1, P_2, \ldots, P_m$ with horizontal axes. There is a global finite bound m on the number pieces. There is strong numerical evidence that $m = 15$, like shown in the picture, and thus, every such polygon consists of (at most) 58 pieces, taken from the grid parabolas $P_1, P_2, \ldots, P_{15}$.

D Experiments with grid peeling for parabolas

Our work was initiated by experimentally exploring the grid peeling process for parabolas $\Pi\colon y = ax^2 + bx$, i.e., parabolas with a vertical axis. These experiments were carried out in the M. Ed. thesis of Moritz Rüber [15], and we report some of the findings from this thesis.

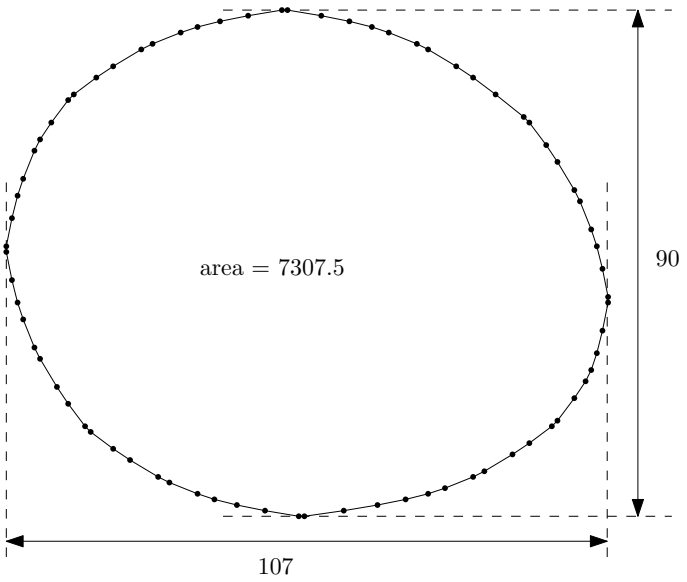

Figure 11: The lattice 75-gon with smallest area, computed by a dynamic-programming approach, see [12, A070911] the Online Encyclopedia of Integer Sequences. The optimal 75-gon is unique up to unimodular transformations.

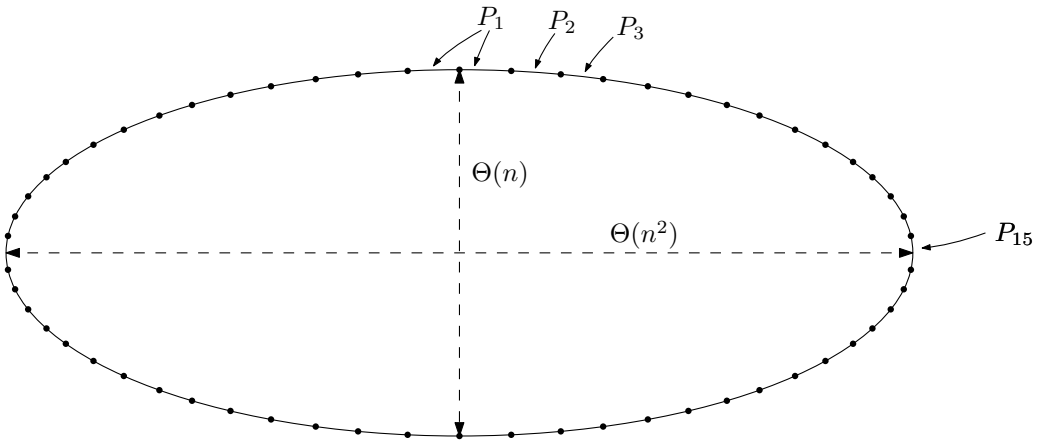

Figure 12: As n increases, the minimum-area lattice n-gon becomes more and more oblong.

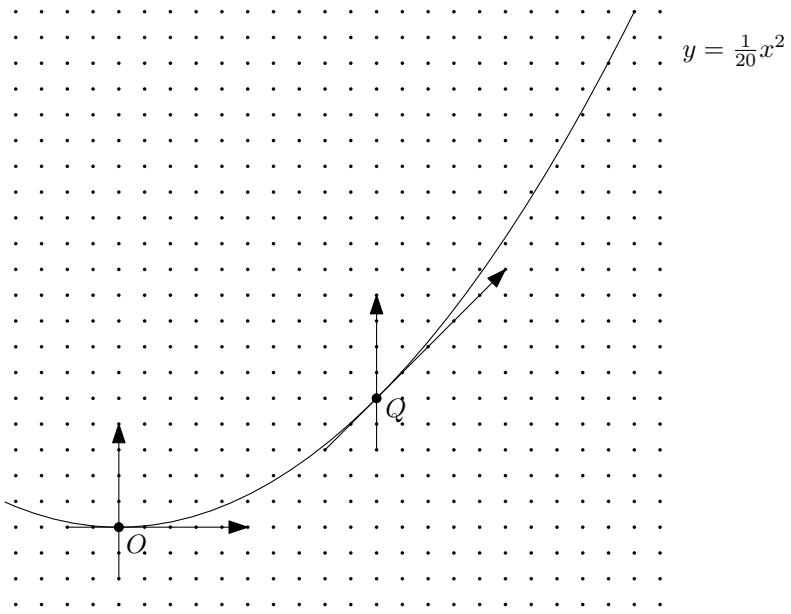

Figure 13: An affine grid-preserving transformations maps the origin O to the point Q and it maps the parabola to itself. The horizontal period H is 10 in this example.

We tried different rational values of a, sometimes in combination with various values of b, and started the grid peeling process. We let the process run until it reached a curve that was a translate of a previous curve, and the process became periodic. Then we could estimate the average vertical speed as well as various other quantities.

In order to carry out these experiments, we needed to restrict the computations to a finite range, as mentioned in the introduction, and therefore we had to compute the horizontal period H: The smallest horizontal translation that, in combination with a shearing operation, maps both the parabola Π and the integer grid to itself. The following lemma, which is analogous to Lemma 1 for the grid parabola, gives a formula for H:

Proposition 5. *Consider the parabola*

$$y = \frac{a_N}{a_D}x^2 + \frac{b_N}{b_D}x + c \tag{23}$$

with reduced fractions $\frac{a_N}{a_D}$ *and* $\frac{b_N}{b_D}$*, and let* $\bar{H} := \operatorname{lcm}(a_D, b_D)$.

The horizontal period H is either equal to $\bar{H}$ or to $\bar{H}/2$. In particular

(i) If $a_D \equiv 0 \pmod 4$*, then* $H = \operatorname{lcm}(a_D/2, b_D)$.

(ii) If $a_D \equiv 2 \pmod 4$ *and* $b_D \equiv 2 \pmod 4$*, then* $H = \operatorname{lcm}(a_D/2, b_D/2)$.

(iii) In all other cases, $H = \operatorname{lcm}(a_D, b_D)$.

Proof. See Figure 13 for an example. Since vertical lines should remain vertical and vertical distances should remain unchanged, the affine transformation that we are looking for has the form

$$\begin{pmatrix} x \\ y \end{pmatrix} \mapsto \begin{pmatrix} x & +H \\ zx + y & +w \end{pmatrix} \tag{24}$$

for suitable parameters H, z, w. Substituting the right-hand sides of (24) for x and y should leave the parabola equation (23) unchanged. This leads to the following equations for z and w:

$$z = 2\tfrac{a_N}{a_D}H \tag{25}$$

$$w = \tfrac{a_N}{a_D}H^2 + \tfrac{b_N}{b_D}H \tag{26}$$

The additional requirement is that (24) should map integer grid points to integer grid points. This boils down to requiring that H, z, and w are integral.

Thus, the horizontal period that we are looking for is the smallest positive integer H for which the two quantities z and w defined above are integers.

Obviously, the choice $H = \bar{H} := \mathrm{lcm}(a_D, b_D)$ makes both (25) and (26) integral. The remainder of the proof, which is elementary but goes into case distinctions, only amounts to checking whether some smaller value of H also does the job.

We start with an easy observation:

Observation A: If H and z are integers and z is even, then w is an integer iff H is a multiple of b_D.

This can be seen after rewriting the first term of (26), using (25) to express one factor H in terms of z,

$$w = \tfrac{zH}{2} + \tfrac{b_N}{b_D} H \tag{27}$$

If zH is even, then the first term $\frac{zH}{2}$ in (27) is an integer. Therefore, w is an integer iff the second term is also an integer, which is the case iff H is a multiple of b_D.

We make a case distinction based on the parity of a_D:

Case 1: a_D is even: Then, from (25), $z = \frac{a_N}{a_D/2} H$ is an integer iff H is a multiple of $a_D/2$.

Case 1.1: a_D is a multiple of 4: Then H is even, and Observation A implies that w is an integer iff H is a multiple of b_D. Part (i) follows.

Case 1.2: $a_D \equiv 2 \pmod 4$. Then a_N must be odd, because $\frac{a_N}{a_D}$ is reduced.

We distinguish two subcases, depending on the (unknown) value H.

Case 1.2.1: H is odd. In this case, $z = \frac{a_N H}{a_D/2}$ is also odd, and the first term $\frac{zH}{2}$ in (27) is a half-integer (a non-integer multiple of $1/2$). For w to be an integer, the second term $\frac{b_N H}{b_D}$ must also be a half-integer. This is only possible if the factor 2 is contained in the denominator b_D. Then b_N must be odd, because $\frac{b_N}{b_D}$ is reduced. If b_D were divisible by 4, then, since the numerator $b_N H$ is odd, $\frac{b_N H}{b_D}$ could not be a half-integer. Hence the only remaining possibility is $b_D \equiv 2 \pmod 4$. Then $\frac{b_N H}{b_D}$ is a half-integer iff $\frac{b_N H}{b_D/2}$ is an integer, which holds iff H is a multiple of $b_D/2$. The value $\mathrm{lcm}(a_D/2, b_D/2) = \bar{H}/2$ is odd, and therefore it is indeed the smallest viable value of H in this case.

Case 1.2.2: H is even. Then H must be a multiple of $\mathrm{lcm}(2, a_D/2) = a_D$. Observation A implies that w is an integer iff H is also a multiple of b_D. Thus H must be a multiple of $\bar{H} = \mathrm{lcm}(a_D, b_D)$.

Summing up the two subcases, we see that the value $\bar{H}/2$ for Case 1.2.1 is indeed the smallest value of H when this case is possible, i.e., when $b_D \equiv 2 \pmod 4$. This establishes Part (ii) of the Proposition. When Case 1.2.1 does not apply, the value $H = \bar{H}$ is in accordance with Part (iii).

Case 2: a_D is odd: Then z is an integer iff H is a multiple of a_D, and z will be even. As above, Observation A implies that w is an integer iff H is also a multiple of b_D. The smallest possible value H is $\bar{H} = \mathrm{lcm}(a_D, b_D)$, and this is in accordance with Part (iii). □

D.1 Results of the experiments

Parabola $y = ax^2 + bx$ for various rational values a and b. We computed the convex hull of the grid points above the parabola and started to peel. After some preperiod, the peeling process will settle into a cyclic behavior: After a certain number Δm of steps, the same curve reappears, translated upward by Δy. We call Δm the *time period* and Δy the *vertical period*. The *average (vertical) speed* v is then $\Delta y / \Delta m$. Figure 14 shows the average vertical speed depending on a (for various values of b).

These experiments show a very clear picture. For almost all a, the average speed takes one of the values $1, \frac{1}{2}, \frac{1}{3}, \ldots$, and it does not depend on b. The sharp transitions between the values occur at *critical values* of a, which we can recognize, with hindsight, as $1/(2H_t)$. In fact, this is

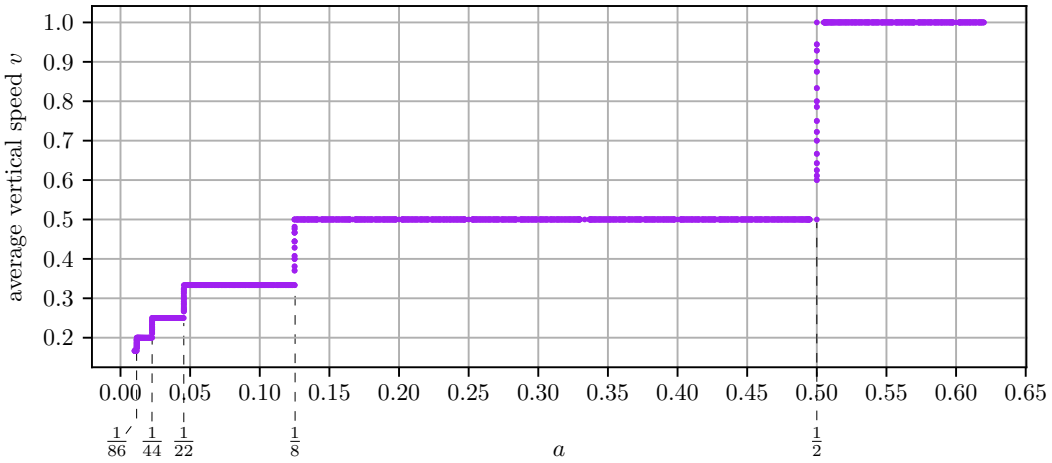

Figure 14: The average vertical speed v of the parabola $y = ax^2 + bx$ versus the coefficient a (for various values of b).

how the phenomenon described in Section 2 was discovered: The sequence of denominators of the critical values $\frac{1}{2}, \frac{1}{8}, \frac{1}{22}$, etc., after clearing the common factor 2, appears in the O.E.I.S. [12, A174405], where various formulas are given, including (9) and (10) in Section A. By trying to find an interpretation of these formulas that would make sense in the context of a convex curve, we were led to the discovery of the grid parabolas P_t. Experiments soon revealed their remarkable behavior under grid peeling, as described in Theorem 2.

D.2 The average speed at the critical values of a

At the critical values $a = \frac{1}{2H_t}$, the average vertical speed varies between the consecutive fractions $\frac{1}{t+1}$ and $\frac{1}{t}$. Figure 15 shows the average vertical speed for the first four critical values a, depending on b. We see a very regular, piecewise linear dependence on b, filling the range between $\frac{1}{t+1}$ and $\frac{1}{t}$.

The horizontal periodicity of these graphs can be explained easily:

Proposition 6. *The parabolas $y = ax^2 + bx$ and $y = ax^2 + b'x$ with $b' = b + 2a$ have the same average speed.*

Proof. See Figure 16. The "shape" of the parabola depends only on a. Variation of b can be interpreted as a translation, placing the vertex of the parabola to a different location. More precisely, the vertex of $y = ax^2 + bx$ lies at the minimum of the function, $x = -\frac{b}{2a}$. Thus, increasing b by $2a$ incurs an amount of horizontal translation that is integral. By Proposition 3, the resulting parabola has then the same average speed. □

We see that the graph consists of H_t repetitions of a sawtooth. Proposition 6 explains the periodicity with period $1/H_t$. It is also clear exchanging b with $-b$ performs only a reflection at the y-axis and thus has no effect on the average vertical speed. This mirror symmetry, together with the periodicity with period $1/H_t$ implies that the whole graph is determined by the part in the interval $0 \le b \le \frac{1}{2H_t}$.

What remains is the remarkable fact that the average speed grows linearly in this interval. We have no explanation for this phenomenon.

The acute observer may notice irregular gaps in the dotted lines of Figure 15. These gaps are, however, only an artifact of the way how the values b were chosen: We took all reduced fractions $b = \frac{b_N}{b_D}$ with $0 \le b_N \le b_D \le 50$. Such a set leaves gaps around values with small denominator like $1, \frac{1}{2}, \frac{1}{3}, \frac{2}{3}$, etc., while it fills other intervals more densely. (In Figure 18 below,

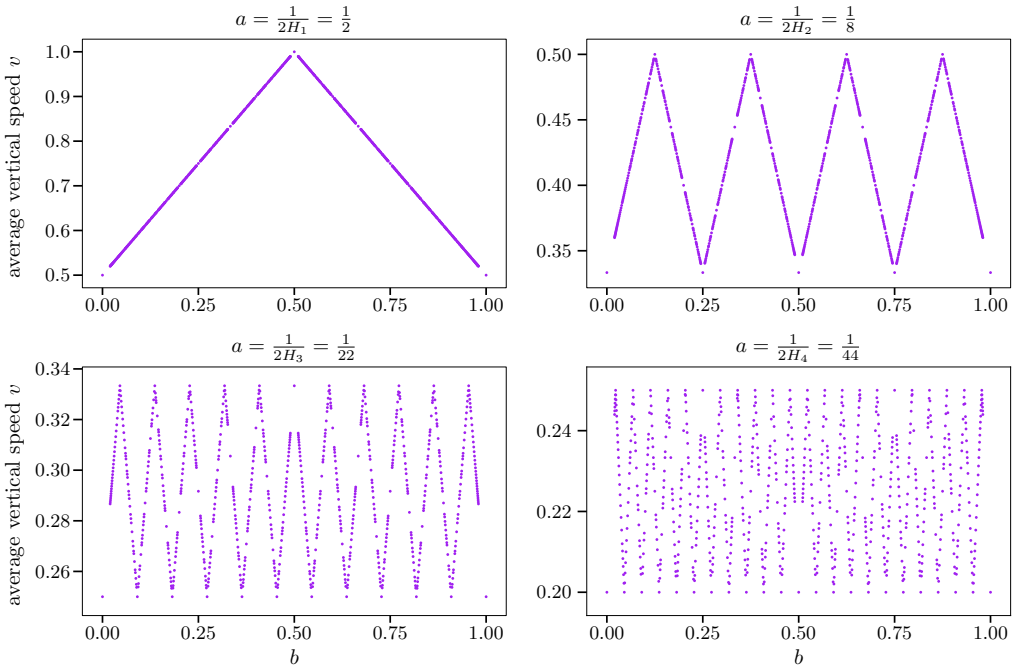

Figure 15: Average vertical speed for critical values $a = \frac{1}{2H_t}$ for $t = 1, 2, 3, 4$, depending on b

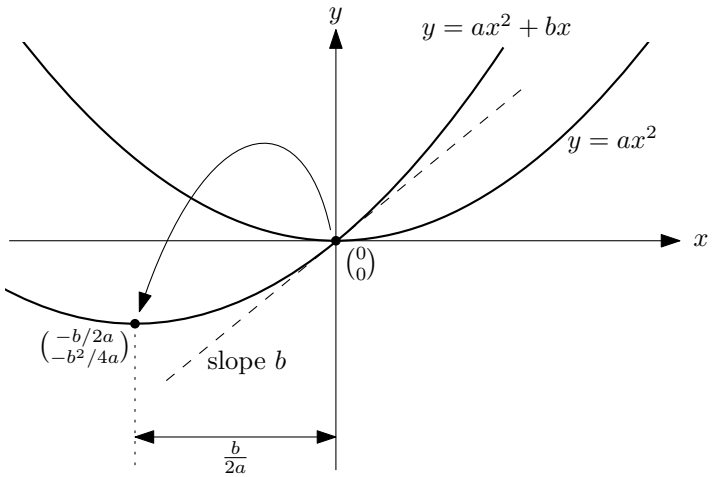

Figure 16: Changing the parameter b of the parabola $y = ax^2 + bx$ amounts to a translation.

this choice of parameters is also the reason why the lower parts of the figure do not exhibit the periodicity of Proposition 3, but rather show the data points arranged along various curves.)

D.3 The time period at the critical values of a

Note that an average speed like $0.4 = 2/5$ (as for the parabola $y = \frac{1}{8}x^2 + \frac{1}{5}x$, for example) means that we can no longer have a vertical period of 1: To get the fraction $2/5$, the vertical period Δy must be a multiple of 2, and the time period Δm must be a multiple of 5. In this example, the true periods are $\Delta y = 6$ and $\Delta m = 15$, see Figure 17. We can see that the curve reappears already after 3 iterations, combined with a horizontal shift by 4 units. Some characteristic pieces of the curves are marked in red in Figure 17 to highlight this repetition. Note that the appearance as a *translation* is due to the special drawing style of Figure 17, which makes also the horizontal period H appear as a translational symmetry. What appears as a translation is actually an affine transformation.

The horizontal period is $H = 20$, and thus, after $20/4 = 5$ shifts (and $5 \times 3 = 15$ iterations), the shifted curve coincides with the original curve, completing a cycle.

This pattern seems to hold for most examples: The curve returns after a "subperiod" of $\binom{t+1}{2}$ steps, shifted by a multiple of H_t, and all multiples of H_t modulo H appear as shifts. Thus, the time period Δm, under these assumptions, is equal to

$$\Delta m = \binom{t+1}{2} \frac{H}{H_t} = \frac{t(t+1)H}{2H_t}, \tag{28}$$

where the horizontal period H is given by Proposition 5. Figure 18 shows the time period Δm for the same set of parabolas as Figure 15, on a logarithmic scale.

For the cases when b is a multiple of a, where the vertical speed takes the "extreme" values $\frac{1}{t+1}$ or $\frac{1}{t}$, the time period is $t+1$ or t respectively, with $\Delta y = 1$. For all remaining cases with one exception, the estimate (28) predicts the correct value. The exception is the parabola $y = \frac{1}{44}x^2 + \frac{1}{5}x$ and its symmetric twin $y = \frac{1}{44}x^2 + \frac{4}{5}x$ with $\Delta m = 25$, whereas (28) would give $\Delta m = 50$. The reason behind this exceptional behavior is that the curve reappears already after 5 iterations (with a horizontal shift of 44) instead of $\binom{t+1}{2} = \binom{5}{2} = 10$ iterations. We suspect that such exceptions will turn up more frequently when more values of b and higher values of t are tested.

In any case, the experiments revealed interesting patterns in the grid peeling process for parabolas (extending the results stated for grid parabolas in Theorem 2 and Lemma 5), The precise structure of these patterns remains to be discovered and analyzed.

We tried to see whether the grid parabola P_t appears when peeling is started with an appropriate parabola. To obtain the time period predicted by Theorem 2, as suggested by the data of Figure 18, we tried the parabolas $y = \frac{1}{2H_t}x^2 + \frac{1}{2H_t}x + \gamma$ for odd t and $y = \frac{1}{2H_t}x^2 + \gamma$ for even t, introducing some vertical shift γ. These parabolas have also the correct horizontal period $H = H_t$ by Proposition 5, using the fact that H_t is even iff t is even (Proposition 1.2).

We found that, although the average speed does not change with γ, the periodic cycle which the process enters can change. For $t \leq 5$, we always found P_t among one of the periodic cycles, with an appropriate choice of γ.

If the piecewise linear dependence of the average speed that is shown by the experiments holds for all values of b, this means that there must be parabolas with an irrational average speed, namely when b is irrational. This would imply that the peeling process is necessarily aperiodic (a statement that can of course not be confirmed experimentally).

D.4 Deviation from the parabolic shape

For a curve C that arises in the peeling process of Π we can compute the deviation from the shape of the starting parabola Π as follows: We find the highest translate $\Pi + \gamma$ that lies below C

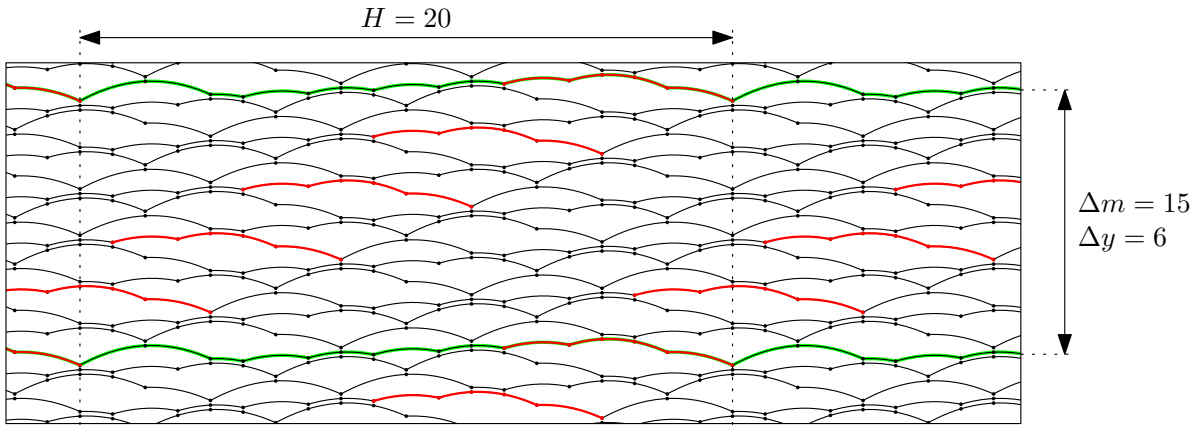

Figure 17: Grid peeling of the parabola Π: $y = \frac{1}{8}x^2 + \frac{1}{5}x = \frac{1}{2H_t}x^2 + \frac{1}{5}x$ for $t = 2$, after the periodic behavior has started. Each curve C is regarded as a function $C(x)$ of x, and we draw the function $C(x) - (\frac{1}{8}x^2 + \frac{1}{5}x)$ instead of $C(x)$. Straight segments have turned into downward-curving parabolic arcs. The original parabola Π would appear as a horizontal line. (This is the same drawing convention that was used for the grid parabolas in Figure 20.)

and the lowest translate $\Pi + \gamma'$ that lies above C, such that C is contained in a parabolic tube of (vertical) thickness $\gamma' - \gamma$.

We looked at all parabolas $y = ax^2 + bx$ with rational coefficients a and b in the interval $0 \le a, b < 1$, where the denominator of a ranges between 1 and 100, and the denominator of b between 1 and 10. For each parabola, we observed the maximum tube thickness of all curves arising during the periodic part of the peeling process. Figure 19 plots the maximum tube thickness on a logarithmic scale and the parameter a. The dependence on b is not shown.

Most of the time, the tube thickness is near 1. Interestingly, it rises to high values when a is close to one of the critical values $\frac{1}{2H_t}$, seemingly approaching a vertical asymptote. At the critical values themselves, the tube thickness is, however, lower than usual.

E Vertical difference between the grid parabola and the reference parabola

For some selected values of t, we have computed the vertical difference $P_t - \Pi_t$ as a function of x, and we show the result in Figure 20.

We observe that P_t is always above Π_t, with the exception of the horizontal segment of length t around the origin. We can clearly discern local minima near $H_t/2$, $H_t/3$ and $H_t/4$, and less marked minima near other rational multiples of H_t.

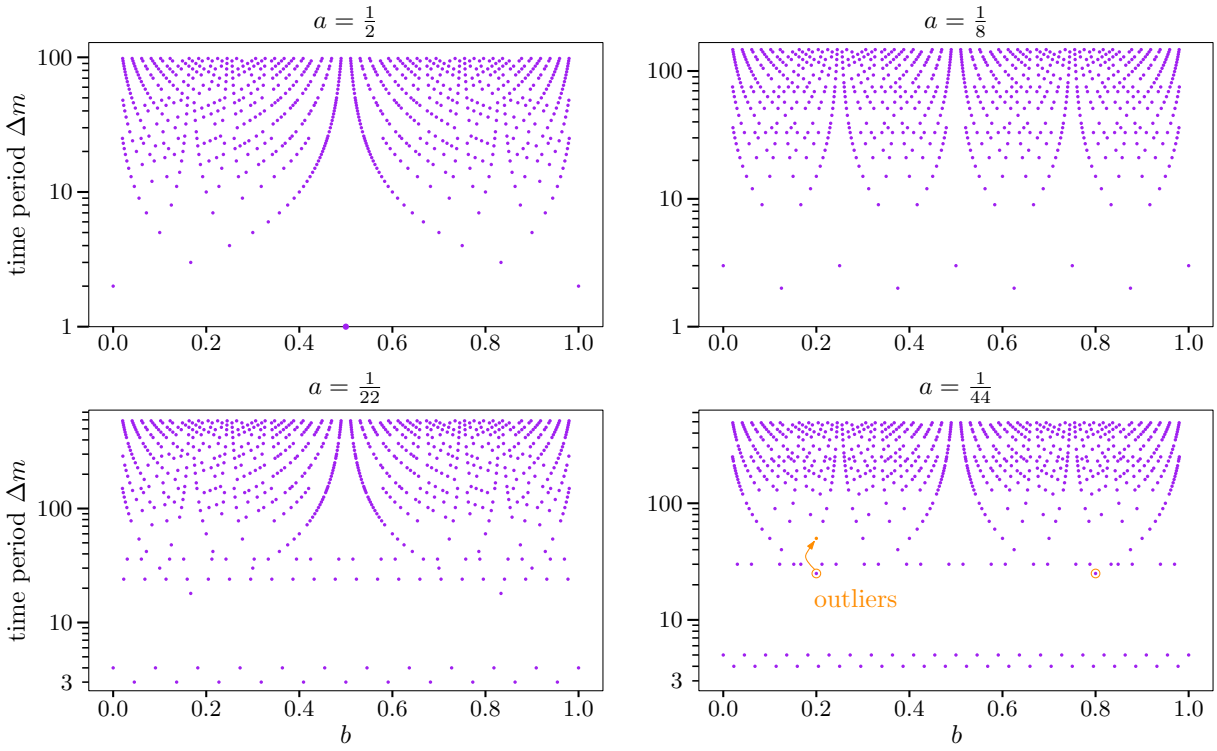

Figure 18: Time period at the critical values a, as a function of b. The orange point in the graph for $a = \frac{1}{44}$ shows where the value should be if formula (28) were true.

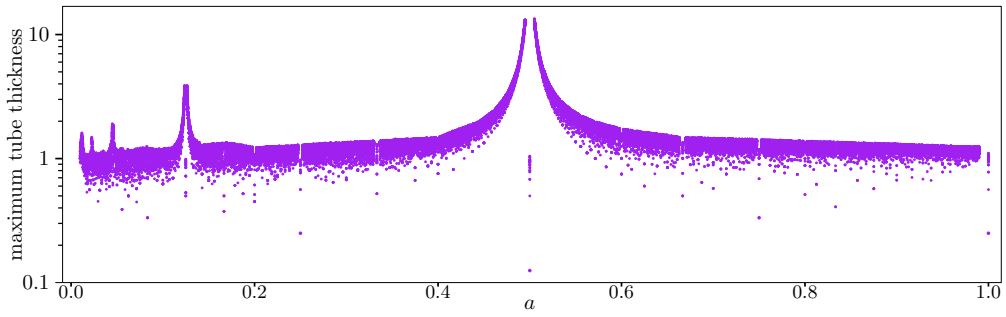

Figure 19: The tube thickness versus the coefficient a, for various values of b.

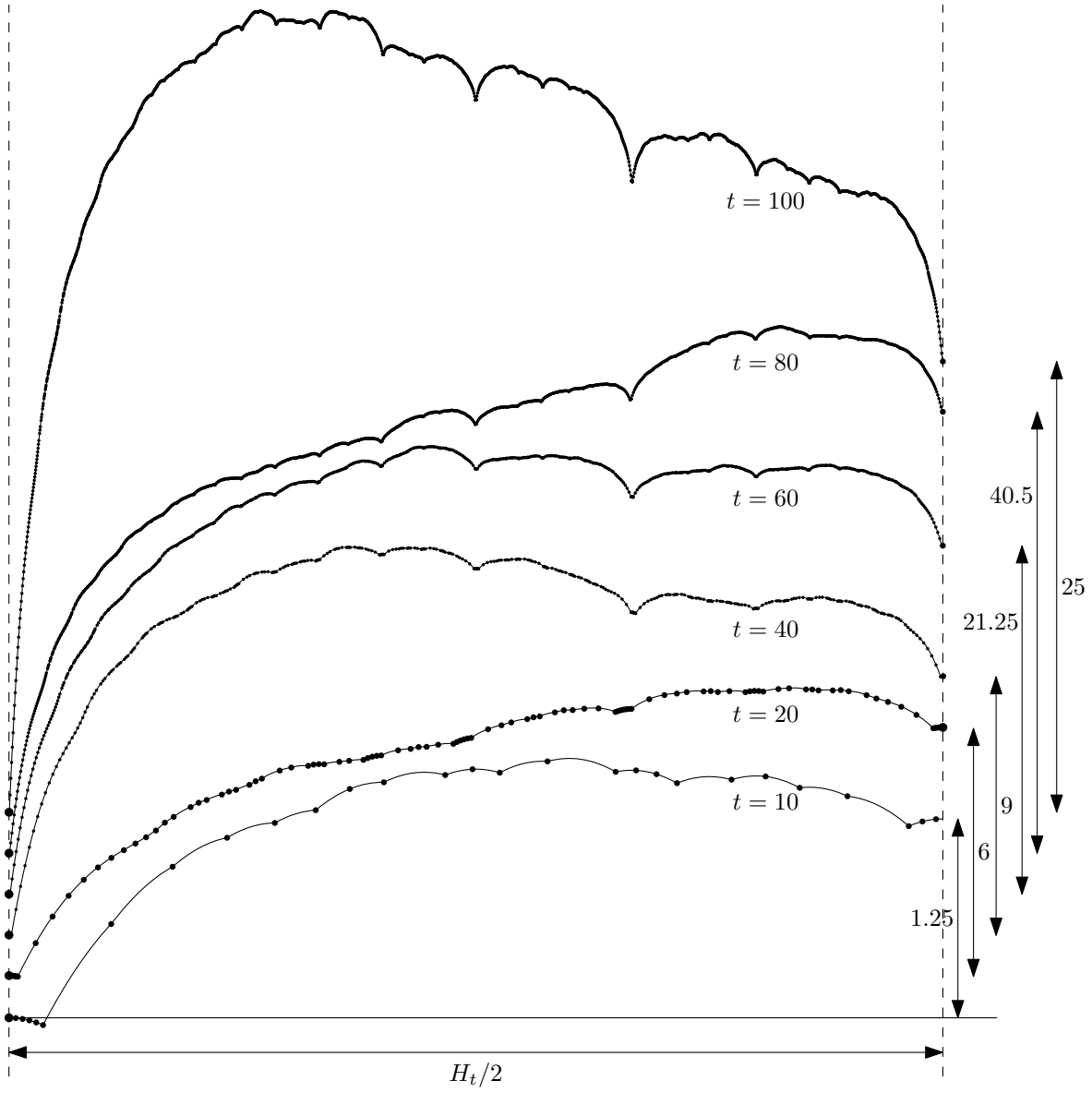

Figure 20: Vertical difference $P_t - \Pi_t$ for $t = 10, 20, 40, 60, 80, 100$. The horizontal axis ranges from the origin to the point $x = H_t/2$, where both P_t and Π_t have slope $\frac{1}{2}$. The boundaries of this interval, marked by dashed lines, act as vertical mirrors for the function $P_t - \Pi_t$. The curves are vertically shifted so that they can be nested under each other, and the vertical scale is chosen independently for each curve: The vertical double-headed arrows show the range between 0 and the difference at $x = H_t/2$. The outlier value 40.5 for $t = 80$ is no mistake. The curve for $t = 80$ rises indeed to a higher maximum than for $t = 100$.